Revised and submitted to: GSA Special Paper "Active tectonics and seismic hazards of Puerto Rico, the Virgin Islands, and offshore areas", editor P. Mann

Towards an integrated understanding of Holocene fault activity in western Puerto Rico: constraints from high-resolution seismic and sidescan sonar data

N. Grindlay[1*], L. Abrams[1], L. DelGreco[1] and P. Mann[2]

[1]Center for Marine Science, University of North Carolina Wilmington, Wilmington, NC 28409

[2]Institute for Geophysics, University of Texas at Austin, Austin, TX 78759-8500

*Corresponding author, email: grindlayn@uncw.edu

ABSTRACT

It has been postulated that the western boundary of the Puerto Rico-Virgin Islands microplate (PRVI) lies within the Mona Passage and extends onland into southwestern Puerto Rico. This region is seismically active, averaging one event of magnitude 2.0 or larger per day, and over 150 events of magnitude 3.0 or greater occurred during the past five years. Moreover, there have been at least 13 historical events of intensity VI (MM) or greater in the last 500 years. We conducted a high-resolution seismic and sidescan sonar survey of the insular shelf of western and southern Puerto Rico during May 2000, in an effort to identify Holocene faults and to further assess the seismic hazard in the region. We focus on a ~175 km^2 part of the surveyed area offshore of western Puerto Rico, extending from Punta Higuero to Boquerón Bay. This area was targeted as a likely place to image recent faults, because multi-channel seismic profiles offshore western Puerto Rico show numerous WNW-trending normal and strike-slip faults that offset

Oligocene-Pliocene age carbonate rocks and underlying Cretaceous basement rocks. Analyses of these data identify three zones of active deformation within the survey area: 1) the Cerro Goden fault zone; 2) the Punta Algarrobo/Mayagüez fault zone that lies offshore the city of Mayagüez; and; 3) the Punta Guanajibo/Punta Arenas fault zone. Two of the offshore fault zones, the Cerro Goden and Punta Algarrobo, show strong correlation with fault zones onland, Cerro Goden and Cordillera, respectively. Many of the mapped faults offshore appear to reactivate older WNW trending basement structures and show evidence of some component of right-lateral motion that is consistent with geodetic measurements. The offshore deformation zones are also associated with headlands and linear NW-SE magnetization lows (serpentinite dikes?) mapped offshore. Elongate outcrops of serpentinite in western Puerto Rico are colinear with the fault zones we have mapped offshore, suggesting that either the presence of serpentinite has localized fault activity or that fault activity has remobilized serpentinite. This offshore study improves assessments of the seismic hazard in Puerto Rico by identifying targets for onshore paleoseismic studies and by better defining the total length of offshore Holocene faults.

Keywords: Holocene faulting, tectonics, Puerto Rico, sidescan sonar, high-resolution seismic reflection.

INTRODUCTION

The onshore and offshore region of western Puerto Rico is one of the most seismically active regions beneath the island of Puerto Rico. During the past five years alone, over 150 earthquakes with a magnitude of 3.0 or greater have been recorded by the local seismic network in the western region of Puerto Rico (University of Puerto Rico (UPR) Seismic Network, unpublished

data). There is historical evidence for at least 48 felt seismic events in the Mona Passage and western Puerto Rico between 1524 and 1958, thirteen of which had estimated intensities of > VI (Modified Mercalli) (Ascencio, 1980). Most notable is the 1918 (estimated 7.3 Ms) earthquake in the Mona Passage (Figs. 1 & 2) and the resulting tsunami, which together killed at least 116 people and caused four million dollars in damage in northwestern Puerto Rico (Reid and Taber, 1919), at a time when the population of Mayagüez was about 17,000 people. Today, Mayagüez is the third most populous city on the island of Puerto Rico with more than 150,000 inhabitants.

Because southwestern Puerto Rico is characterized by "basin-and-range" style topography and frequent shallow (<50 km) seismicity (McCann et al., 1987; Joyce et al., 1987; Ascencio, 1980; UPR seismic network, unpublished data), this region has been the focus of studies to locate Holocene faults onland. Two seismic reflection lines across the southern margin of the Lajas valley imaged displacements in Quaternary lacustrine sediments and Cretaceous basement rocks (Meltzer, 1998; 2000). Offsets within the sediments and the basement rocks indicate Quaternary faulting, most likely of a transtensional nature (Meltzer, 1998; 2000). Most recently, trenching studies of the South Lajas fault near the town of Boquerón showed evidence of Holocene activity (Fig. 3). Displacements in Holocene alluvium show valley-side down, normal separation with a component of strike-slip motion (Prentice and Mann, this volume).

Marine geophysical studies of the Mona Passage indicate several sets of youthful, large displacement, normal faults (Gardner et al., 1980; Larue and Ryan, 1990; Grindlay et al. 1997; van Gestel et al., 1998). The Mona rift, located at the northern end of the Mona Passage (Fig. 1& 2), is a N-S trending graben with extremely large throws, in many instances over 2 km (Gardner

et al., 1980; Larue and Ryan, 1990; Grindlay et al., 1997; van Gestel et al., 1998). Recent tectonic activity in the area is suggested by uneroded rocks on the fault scarps, and by normal faults and vertical fissures which cut tilted surface layers (Gardner et al., 1980). South of the Mona rift, single-channel (SCS) and multi-channel seismic (MCS) data show an abundance of normal faults with generally WNW and E-W trends (Western Geophysical Company and Fugro, Inc., 1973; Larue and Ryan, 1990; Grindlay et al., 1997; van Gestel et al., 1998; 1999; Fig. 2).

Because most of the large historical earthquakes have been located far offshore, and existing nearshore geophysical data is sparse, an understanding of the distribution and nature of nearshore faults and the seismogenic potential on the insular shelf of western Puerto Rico is lacking. For this reason, we conducted a high-resolution geophysical survey (SCS and sidescan sonar imaging) in May 2000 to characterize the structure of the seafloor and sub-bottom of the shallow insular shelf (Fig. 3). The primary objective of this study was to search for youthful faulting (e.g., seafloor offsets), and to correlate offshore faults with possible Quaternary faults mapped onshore to better define their total length in western Puerto Rico. The delineation of nearshore fault systems provided by this study, combined with their direction and rate of slip from onland surveys, will assist in the improvement of hazard models. Until now, hazard models have relied only on offshore source zones for hazard prediction, because of the lack of evidence for nearshore and onshore faulting.

TECTONIC SETTING OF PUERTO RICO AND THE VIRGIN ISLANDS

The island of Puerto Rico is located within a diffuse and complex plate boundary zone between the North American and Caribbean plates (Fig. 1). Seismicity and marine geophysical

studies suggest that Puerto Rico and the Virgin Islands are the emergent part of a microplate that lies within the North American-Caribbean plate boundary zone (Byrne et al., 1985; Masson and Scanlon, 1991; Mann et al., 1995). The Puerto Rico trench and the Muertos trough form the northern and southern boundaries, respectively, of the Puerto Rico-Virgin Islands (PRVI) microplate (Fig. 1). The eastern boundary of the microplate lies within the Anegada Passage. The western boundary of the microplate is poorly defined; its northern portion may be the Mona rift, while its southern portion may lie beneath the Mona Passage or extend into southwestern Puerto Rico.

Phases of deformation impacting the region

It is likely that the style, geometry and distribution of faults within the Mona Passage and western Puerto Rico are a function of at least three separate and sequential phases of deformation to impact this region. The first phase is an Eocene age transpressive event focused along two major shear zones the Great Northern Puerto Rico fault zone (GNPRFZ) and the Great Southern Puerto Rico fault zone (GSPRFZ) (Erikson et al., 1990, 1991; Figs. 1 & 2).

The second phase of deformation of N-S shortening occurred in response to post-Eocene-Neogene convergence between the North American and Caribbean plates (Dillon et al., 1994; Van Gestel et al., 1998). The episode of deformation resulted in a broad, 120-wide arch that has an axis that extends from eastern Hispaniola through the Mona Passage to the western side of the island of Puerto Rico (van Gestel et al., 1998) (Figs. 2 & 3). Localized extension at the crest of the arch presumably caused many small faults with a range of orientations, including many E-W trending normal faults.

The third, and on-going phase of deformation is characterized by extension in the Mona Passage and possibly western Puerto Rico. The extension is believed to be caused by the differential ENE relative motion of the PRVI with respect to eastern Hispanoila (Grindlay et al., 1997; van Gestel et al., 1998; Jansma et al., 2000; Mann et al., 2003). The extension could be accommodated by reactivation of WNW trending normal faults or shear zones developed during previous deformational phases. Recently published GPS geodetic measurements collected during a 10-year period in the region suggest that the amount of differential motion between Hispanoila and Puerto Rico is about 5 mm/yr (Lopez et al., 1999, Jansma et al., 2000; Mann et al., 2003). Geodetic studies also suggest that Puerto Rico and the Virgin Islands are currently behaving as part of the stable Caribbean plate and are moving in a ENE direction (~070°) at a rate of 19-20 mm/yr relative to North America (Jansma et al, 2000; Mann et al., 2002; Fig. 1).

GEOPHYSICAL DATA COLLECTION AND PROCESSING

We conducted a 10-day marine geophysical survey using the University of Puerto Rico's R/V *Isla Magueyes* in May 2000. We surveyed extensively (728 line km of data) the insular shelf off of western Puerto Rico, from Punta Higuero to Cabo Rojo (Fig. 3). Sidescan sonar and high-resolution sub-bottom profiler data were acquired simultaneously and merged with Differential Global Positioning Satellite (DGPS) navigation ($\pm$5m resolution). Surveying extended very close to shore in water depths as shallow as 2 m, increasing our ability to correlate with known onshore faults. Trackline spacing was ~300 m. The sidescan sonar system generated 300 to 400 m-wide swaths of 100 kHz and 500 kHz seabed reflectivity data, which were later assembled into mosaic images with 1 m pixel resolution. All of the sonographs have been filtered, slant

range corrected, bottom corrected, destriped and beam-angle corrected before being placed into a georeferenced digital mosaic. The SCS boomer system operated at 280 Joules and 2 shots per second. At the average ship speed of 5 kts, this resulted in a shot spacing of approximately 1.3 meters. The SCS data have been processed as shown in Table 1. Vertical resolution is estimated at 1 m, and penetration ranged from only imaging the seafloor in reefal areas to over 100 milliseconds below the seafloor (msbsf) in areas where relatively thick accumulations of unlithified alluvium were present.

Existing seismic data

MCS data were acquired in 1972-1973 by Western Geophysical Company and Fugro for the Puerto Rico Water Resources Authority (Western Geophysical Company of America, and Fugro, Inc., 1973). MCS profiles separated by 5 to 10 km surround the island and were collected in a site assessment for a nuclear power plant. The MCS data were acquired with a 24-channel streamer with 67 m group spacing, and were digitized and recorded using a SDS 1010 system. After acquisition, these data were processed using a single deconvolution operator, limited velocity analyses, and stacking. The MCS data set is owned by, and stored at, UPR as large-scale paper and mylar records. We digitally scanned and examined the limited number of MCS lines that cross or coincide with our shallow water survey of the inner shelf. In addition, we have used one MCS line that has been reprocessed to include migration (Detrich, 1995; Fig. 4). Initial reports provided by Western Geophysical Company and Fugro (1973) indicate an abundance of faults that cut deeply into or through the Oligocene-Pliocene carbonate platform off western Puerto Rico. We have used mapped traces of these faults, projected to the surface as originally

proposed by Western Geophysical Company and Fugro (1973), where they could be verified by re-inspection of the original MCS data.

SEISMIC STRATIGRAPHY AND GEOLOGY OFFSHORE WESTERN PUERTO RICO

U.S. Geological Survey marine geologic maps based on grab and dive samples and 3.5 kHz seismic records show surface sediment thickness ranging from <1 to >10 m (Grove, 1983; Schlee et al., 1999) on the western insular shelf of Puerto Rico. Seafloor sediment composition is mixed terrigenous and skeletal sand and mud nearshore, and mostly carbonate mud further offshore, punctuated by carbonate hard grounds and shallow reefs (Grove, 1983; Schlee et al., 1999). Presently, the Añasco River deposits siliciclastic material in the nearshore environment resulting in relatively thick (up to100 m) local accumulations of siliciclastic sediments. The age of the unlithified material imaged by SCS data is unknown, but is inferred to be primarily alluvium deposited since the last sealevel low-stand (i.e. Holocene) on an erosional (often hardground) surface.

The insular shelf to slope break within the study area is marked by an almost continuous line of submerged coral reefs that rise to water depths of 15-20 m. The entire insular shelf and upper slope were exposed to subaerial erosion from before 15,000 years until after 10,000 years ago (Morelock et al., 1994). In the southwest along the Parguera shelf (Fig. 2), the Holocene shelf-edge reefs began growing 8,000 to 9,000 Ka on the newly submerged Pleistocene surface (Morelock, 1994 Hubbard et al., 1996). These coral died off 6,000 Ka and the surface was barren until massive coral began to grow a few hundred years ago (Morelock, 1994; Hubbard et al., 1996).

Underlying the Holocene sediments is a thick (up to 1500m) Oligocene-early Pliocene age sequence of shallow-water limestone that lies unconformably over Cretaceous-Eocene volcanics (Moussa et al., 1987). It is assumed that these carbonates are contiguous with the tilted carbonate sequences that extend offshore on the northern and southern insular slopes of the islands (Moussa et al., 1987; van Gestel et al., 1998). The tilted platforms of opposing dip are interpreted to be limbs of a roughly east-west trending, 120 km-wide arch that resulted from a north-south shortening event (Phase 2 described in section II) from post Eocene to late Neogene (Dillon et al., 1994; van Gestel et al., 1998). The MCS profile shown in Figure 4 images the northern limb of this arch. Existing MCS profiles offshore western and southern Puerto Rico, collected by Western Geophysical Company and Furgo, show numerous E-W and WNW trending normal and strike-slip faults offsetting the carbonate platform strata and the underlying Cretaceous-Eocene volcanic basement (Larue and Ryan, 1990).

The primary limitation of these MCS data for this study is the lack of resolution of structure in the uppermost sediments and the limited coverage in shallow water. The high-resolution SCS profiles from our survey, therefore, complement the existing MCS profiles collected by Western Geophysical Company and Fugro, Inc. SCS profiling of carbonate hard grounds and reefs resulted in high-amplitude seafloor reflections with very limited sub-seafloor penetration along with significant seafloor multiples obscuring any possible sub-bottom structure. Sediment thicknesses of less than 1 m, which is often the case, were not resolvable. In other locations, sediment stratigraphy is well imaged above a relatively high-amplitude reflection(s) forming acoustic basement, interpreted to be the top of the carbonate platform strata. Acoustic basement

on SCS data often appears as a uniformly dipping reflection or series of reflections beneath onlapping and/or draping, semi-continuous, relatively flat-lying reflections to hummocky clinoforms. In other areas, stratigraphic relationships indicate acoustic basement was affected by cut and fill processes.

For the purposes of this study, youthful faulting is identified by displacements of the seafloor and within the uppermost, unlithified (Holocene?) sediment, lying unconformably over the faulted carbonate platform and/or linear disruptions of the sediment at the seafloor observed on the sidescan sonar mosaics.

OBSERVATIONS AND INTERPRETATIONS

In this section we present the observations and interpretations of the sidescan sonar and SCS data collected during the May 2000 cruise. Data are presented in four geographic regions (Fig. 3): the North Añasco Bay region, the North Mayagüez Bay region, South Mayagüez Bay region and the Boquerón Bay region.

North Añasco Bay region

The sidescan sonar mosaic of the northern Añasco Bay (Fig. 5) shows a low reflectivity area on the ~3km wide insular shelf near the mouth of the Añasco River. The areas of low reflectivity are interpreted to be deposits of fine-grained sediments, mainly mud and sands (Grove, 1983). The areas of high and chaotic reflectivity near the shelf edge are interpreted as unsedimented reefs. The shelf becomes narrower (<1 km) and more reef- and reef debris-dominated to the north, indicated by more and larger areas of high and chaotic reflectivity. The

shelf edge parallels the coastline, and south and west of Punta Cadena the seafloor drops off rapidly to depths in excess of 300 m. Two parallel, curvilinear, high-reflectance features that are separated by 200-300m are clearly visible in the sidescan sonar mosaic (Figs. 5 & 6). These linear features parallel the coastline as it changes trend from northeast-southwest, north of Punta Cadena to roughly east-west, south of Punta Cadena. Seismic profiles (Fig. 6) show two areas of steeper slope ~10-15 m high, at ~80 m and ~40 m depth, which correspond to the location of the highly reflective linear features seen on the sidescan sonar mosaic. It has been suggested that the during the last transgression, sea level rise either stopped, slowed dramatically or even dropped to form paleo-shores (e.g., mid-Atlantic continental shelf, Emery and Uchupi, (1984)). We hypothesize that the two "steps", or terraces, imaged on the slope represent stillstands or slow downs in sea-level rise where reefal growth was able to keep pace with sea-level rise. These submerged terraces are comparable to the submerged reefs found at 20 m water depths at the edge of the insular shelf. Most importantly, offsets in these linear features can be used to pinpoint locations of youthful faults offshore and potentially determine sense of relative motion along the fault trace.

Shore-parallel SCS lines just seaward of the Añasco River reveal the thickest sections (>100ms) of continuous flat-lying reflections that onlap and bury reef-like pinnacles, sometimes display cut and fill geometries and occasionally are severely attenuated, presumably the result of gas-charged sediments. This seismic facies is interpreted as well-stratified alluvium from the Añasco River. These deposits thin and extend to the northern, east-west trending, shore where they appear as relatively thick (25 m) accumulations between shallow reef heads. Several of our high-resolution SCS profiles (Fig. 7) clearly show displacements of the seafloor and these

alluvial sediments that we interpret to be Holocene age.

On the basis of the SCS, sidescan sonar and bathymetry data, we have identified parallel, semi-continuous fault traces (Figs. 5, 6 & 7) that trend ENE. One of these fault traces (F3, Fig., 5) cuts across the submarine terraces at nearly right angles and appears to offset them in a right-lateral sense. The offset in the reef at 20 m water depth is most clearly distinguishable and is approximately 400 m (Fig. 5, inset). Fault traces can be traced close to shore, but on SCS lines closest to the shore no displacements are observed in the well-stratified and relatively thick sediments.

MCS profiles XI-108D (Fig. 7) and ID-131-D (Fig. 4, north end) cross the narrow shelf south of Punta Cadena and reveal a high angle normal fault offsetting the Oligocene-Pliocene carbonate strata. It is not clear from the MCS profiles if this fault displaces sediments on the seafloor. The map view projection of these deep faults to the seafloor lies within the zone of parallel and semi-continuous fault traces that displace the seafloor and Holocene sediments. This narrow band of faults is interpreted as an offshore portion of the Cerro Goden fault zone (Figs. 3&4).

North Mayagüez Bay region

The sidescan sonar mosaic of the North Mayagüez Bay region (Fig. 8) shows a wider (3-5 km) section of the insular shelf that is dominated by low-reflectivity seafloor that is determined from grab samples to be mainly silty sand and mud (Schlee et al., 1999). Two large areas of chaotic/high reflectivity at the mouth of the bay are interpreted to be reefal areas. The western

edges of the reefs form a semi-circle that is cut at its midpoint by a narrow NW-SE trending channel (Fig. 8). The sidescan sonar mosaic shows an abrupt change in reflectivity along the southern edge of the channel that corresponds to small offsets, down to the south, in the SCS data that project northwestward to a very steep, south facing slope (Fig. 9). West of the shelf edge the seafloor deepens, forming a bowl-shaped basin called the Mayagüez basin (Figs. 4, 8 & 9). In the sidescan sonar imagery we observed at least two linear and parallel, high reflectivity features that follow contours along the southern edge of this basin, which we interpret to be submarine terraces comparable to those observed in North Añasco Bay (Fig. 8). These terraces also appear to terminate at the southern edge of the NW-SE trending channel.

MCS lines running north-south offshore Mayagüez Bay clearly show north dipping reflectors truncated by high-angle, normal faults forming a significant scarp (Figs. 4 & 9). The north dipping reflectors are interpreted to be the Oligocene-Pliocene carbonate platform and the scarp separates the clastic sediment depocenters of Mayagüez Bay and Añasco Bay into two sub-basins: the Mayagüez and Añasco basins (Fig. 4). SCS profiles collected in the Mayagüez Bay area parallel to, and overlapping these MCS lines (Fig. 9) show this scarp as a steep WNW-ESE trending slope, with 50-100 m of relief. Several parallel, high-amplitude reflectors, which dip north at approximately 6˚, terminate at, or near, the surface beneath a thin section of flat-lying continuous reflections. The dip and normal component of fault motion can be seen on the MCS profiles (Fig. 4 & 9B), however, due to their low resolution, it is not clear whether the seafloor or uppermost sediments are disrupted. The SCS profiles also show the north-dipping reflectors truncated by the south-facing scarp near the seafloor and only a thin (<2 m) veneer of sediment at the ridge (Fig. 9A). The thin Holocene (?) sediments on the top of the ridge are consistent with

a recent uplift history, but are too thin to enable offset strata to be seen. Additionally, the lack of piercing points makes determination of the direction and magnitude of strike-slip motion (if any) impossible to determine.

Sidescan sonar imagery shows areas of lower reflectivity 'streaking" down the south face of the scarp (filled arrows - Fig. 8) and along with the SCS data indicates sediment transport through breaks in the reef. SCS profiles show a thick wedge of sediments accumulated at the base of the slope (Fig. 9). Since no river empties directly into Mayagüez Bay, the source of these sediments is interpreted to be the Añasco River to the north. Offsets of this alluvium and seafloor at the base of the scarp align with displacements and terminations of linear seafloor features observed closer to shore in SCS and sidescan sonar data. The set of offsets that project from the head of the scarp landward toward Punta Algarrobo and those that project towards Mayagüez Bay are referred to as Punta Algarrobo and Mayagüez fault zones, respectively (Fig. 4, PA/MFZ).

South Mayagüez Bay region

The sidescan sonar mosaic of South Mayagüez Bay (Fig. 10), on a relatively wide section of the insular shelf (8-10 km), is dominated by highly reflective seafloor interpreted to be large expanses of coral reefs. The highly reflective area is truncated to the north by a NW-SE trending lineament, that marks an abrupt change to lower reflectivity seafloor (muds and sands). Corresponding to this boundary, and visible on adjacent SCS profiles, is a narrow (400m-wide) trough, with a nearly vertical 10 ms offset (down to the south) at the seafloor that trends NW-SE (Figs. 10 & 11). An approximately 20 ms interval of flat-lying, continuous reflections overlying

dipping and diverging reflections terminate abruptly at the north wall of this trough (Fig. 11). This seismic image is interpreted as a relatively thick section (~ 15 m) of well stratified alluvium (Holocene?) that has filled a fault bounded depression which has continued to experience a component of vertical motion since infilling began. In addition, contours marking the submerged reef at the shelf edge (20 m depth) appear to be offset approximately 750 m in the right-lateral sense across the trace of this fault (Fig. 10). Other, smaller vertical offsets of the seafloor and surface sediments are also imaged on parallel and adjacent SCS profiles. The set of parallel and semi-continuous fault traces, trending NW-SE, that project toward Punta Guanajibo, define the offshore section of the Punta Guanajibo fault zone (Figs. 4, 10&11, PGFZ).

Offshore from Punta Arenas, the reefal areas are cut by several discontinuous NW-SE trending lineaments (Punta Arenas fault zone, Fig. 10). The lineaments extend southward into the areas of muds and sands (dark-grey) and silty clays (light grey), but do not correspond to clear offsets of the seafloor in the SCS data. This is not to say that offsets do not exist. Sediment thicknesses in this area are extremely thin (< 1 m, below system resolution) and the hardbottom nature of the seafloor resulted in high-amplitude seafloor reflections with very limited sub-seafloor penetration along with significant seafloor multiples obscuring any possible sub-bottom structure.

Boquerón Bay region

Extensive surveying of the area offshore of the Lajas valley did not reveal any evidence of the South Lajas fault surveyed on land by Meltzer et al. (1998; 2000) and Prentice and Mann (this volume). The sidescan sonar mosaic shows areas of very fine silty clays (light grey) close to shore in Boquerón Bay and in the northern half of the survey area (Fig. 12). Seafloor

sediments consisting of sands and muds (Schlee et al., 1999), seen as dark grey areas in the sidescan sonar mosaic, dominate the southern portion of the survey area. Within Boquerón Bay and at the mouth of the bay, SCS profiles show south-dipping reflectors, which we interpret to be the Oligocene-Pliocene carbonate platform, overlain by the relatively flat-lying reflections interpreted as Pliocene-Holocene sediments (Fig. 13). The presence of dipping reflectors on adjacent profiles with dissimilar azimuths enabled us to calculate a true dip of 3° to the SSW. The dipping reflectors extend to the seafloor where they appear to be truncated along an erosional surface, on top of which lies a thin covering of sediment (Holocene?). The dip of the reflectors abruptly changes to the north on the north side of an E-W trending bathymetric high at 18°06'N. We interpret this change in dip to mark the axis of the regional E-W trending arch (Figs. 3 &12).

DISCUSSION

Evidence for Holocene faulting offshore western Puerto Rico and onland extensions

The systematic sidescan sonar and high-resolution SCS survey of the western insular shelf of Puerto has revealed at least three regions of active deformation.

1) The first region includes the offshore extension of the Cerro Goden fault zone (Figs. 14&15). Onland this fault parallels an abrupt, linear mountain front separating the 270-361 m high La Cadena de San Francisco mountain front from the alluvial Añasco valley (Figs. 3&4). Previous workers have postulated that the Cerro Goden fault zone continues to the southeast as the GSPRFZ and to the west, merges with the normal fault forming the eastern wall of the Mona rift (Garrison and Buell, 1971; McCann, 1985) (Figs. 1 & 15). Onland about 500 m south of the

prominent La Cadena mountain front, Mann et al. (this volume) found geomorphic features suggestive of right-lateral Quaternary fault activity, including offset terrace risers and upslope-facing faults. The projection of the mapped onland trace of the Cerro Goden fault zone offshore lies along the northern edge of Añasco Bay and appears as a set of semi-continuous fault traces indicating Holocene activity (Figs. 5, 6&7). To the north and west of our survey area, MCS profiles indicate that the fault zone extends to the Desecheo Ridge, the southern limit of the Mona rift (Figs. 3 &15).

2) The second zone of deformation is the Punta Algarrobo/Mayagüez fault zone (Figs. 14 & 15). The slope and truncated dipping reflectors that indicate the position of the Punta Algarrobo fault zone are not visible on the SCS profiles nearest to shore due to the thickness of the sediment column resulting from rapid accumulation of alluvium, therefore it cannot be directly linked to faults mapped onshore. However, the similarity in trend, location, and type of motion suggest that the fault zone imaged in the northern Mayagüez Bay area is the offshore extension of the Cordillera fault mapped by Moya (1994), who proposed activity within the Quaternary. The offshore fault zone projects into the WNW-ESE trending Monte del Estado peridotite/serpentinite belt onland (Figs. 3, 14).

3) The third zone of deformation is the Punta Guanajibo/ Punta Arenas fault zone that projects to Punta Guanajibo and Punta Arenas (Figs. 14&15). These areas are characterized by the NW-SE trending Rio Guanajibo serpentinite belt onland (Figs. 3&14). In addition, Moya (1994) identified a WNW trending fault with vertical offsets along the southern flank of the

Cordillera de Saban Alta, the seawardmost unit of the serpentinite belt (Figs. 3 & 14). Moya (1994) suggests that this fault shows Quaternary activity.

Both the Punta Algarrobo/Mayagüez and Punta Guanajibo/Punta Arenas fault zones project to, and are colinear with, the trend of onland serpentinite bodies. The serpentinite bodies are associated with magnetization lows that extend offshore, suggesting that the serpentinite also extends offshore (Fig. 14). The faults mapped offshore in this study correspond to the magnetization lows. This relationship suggests that either the presence of serpentinite has localized fault activity or that fault activity has remobilized serpentinite. In either case the relatively weak and ductile serpentinite may be accommodating part of the strain associated with the regional stress regime by many frequent, small magnitude events, thus accounting for the intense, low magnitude seismic activity that characterizes southwestern Puerto Rico.

The lack of evidence in the offshore for young faulting associated with the South Lajas fault does not necessarily mean there is no Holocene offshore displacement on this structure. This fault has at least a component of strike-slip displacement and is only known to have had two displacement events in the Holocene (Prentice and Mann, this volume). With such a small amount of Holocene displacement, it is possible that it is not resolved even with a high-resolution seismic system, especially if most of the motion is strike-slip. However, the sidescan sonar imagery also failed to detect evidence of the fault, suggesting that if a young fault does exist, recent sedimentation has masked its surfical expression on the seafloor. Alternatively, the South Lajas fault could be one of many short fault segments that, when taken together, form a regional fault system within southern Puerto Rico.

Implications for neotectonics of western Puerto Rico and the Mona Passage

On the basis of previous marine geophysical studies as well as the recent onland and marine studies it is becoming increasingly apparent that the deformational history of Puerto Rico and its vicinity is very complex. One result of our offshore survey and the coordinated onland trenching and mapping studies (Prentice and Mann, this volume; Mann et al., this volume) is to show the presence of several Quaternary faults intersecting the west coast, and that many of these faults appear to be reactivated, older, WNW trending basement structures.

The youthful faults we mapped offshore appear to be largely confined to the northern and central areas of the western Puerto Rico insular shelf. The rugged seafloor morphology in this region reflects this wide zone of deformation (Fig. 15). In marked contrast, the southwestern portion of the insular shelf, where we found little/no evidence of youthful faults, is wide, smooth and flat (Fig. 15). The offshore sections of the Cerro Goden, Punta Algarrobo/Mayagüez, and Punta Guanajibo/Punta Arenas fault zones are all observed to have normal fault geometries, and in the case of the Cerro Goden and Punta Guanajibo fault zones some evidence suggesting right-lateral strike-slip component is observed. The onshore sections of both of these faults also exhibit right-lateral motion of probable Quaternary age (Mann et al., this volume; Moya, 1994). If the faults observed offshore are Holocene, then by their coincidence in location and style of motion with older structures (faults in the Oligocene-Pliocene carbonates) they likely represent reactivation or continued motion on those structures (Fig. 4). The overall stress regime suggested by motion on these faults therefore is extension aligned roughly NE-SW. (Fig. 15b). This is consistent with geodetic studies that suggest ENE extension is occurring in the Mona Passage

and is largely accommodated by the opening of the Mona rift and associated faults (Jansma et al., 2002; Mann et al., 2003), (Fig. 15b).

CONCLUSIONS

In summary, both the offshore and onland studies have documented for the first time evidence suggesting Quaternary fault activity associated with a broad zone of deformation in the Mona Passage and western Puerto Rico. Three fault zones have been identified offshore western Puerto Rico: the Cerro Goden, the Punta Algarrobo/Mayagüez, and the Punta Guanajibo/Punta Arenas fault zones. These faults appear to coincide with large WNW trending offsets in the underlying Cretaceous volcanics and Oligocene-Pliocene carbonate sequences, suggesting that many of these faults represent zones of weaknesses that are being reactivated in the most recent phase of NE-SW extensional deformation. Two of the fault zones, the Cerro Goden and Punta Algarrobo, show strong correlation with fault zones onland, Cerro Goden and Cordillera, respectively. Our studies, coupled with the onland studies of Prentice and Mann (this volume), Mann et al. (this volume) and Hippolyte et al. (this volume) suggest that these faults pose a seismic hazard and must be considered in future seismic hazard models for the island of Puerto Rico, one of the most densely populated regions of the western hemisphere.

ACKNOWLEDGMENTS

We gratefully acknowledge Captain Hector and the crew of the R/*V Isla Magueyes* for their skill and enthusiasm in navigating the shallow reef-invested waters of western and southern Puerto Rico. John "super tech" Murray ensured the smooth operation of the geophysical gear during the cruise. We thank Osku Backstrom and Daniel Lao for watchstanding during the

cruise. Christa von Hilldebrant, Victor Huerfano and other members of the UPR seismic network and the UPR geology Department generously provided time and logistical support for the field work conducted in PR. We thank Carol Prentice and Tom Pratt for their helpful reviews of this manuscript. This research was funded by USGS Grant# 00HQGR0010. UTIG contribution#

REFERENCES CITED

Ascencio, E., 1980, Western Puerto Rico seismicity: U.S. Geological Survey Open-File Report 80-192, 135 p.

Bracey, D.R., 1968, Structural implications of magnetic anomalies north of the Bahama-Antilles islands: Geophysics v. 33, p. 950-961.

Byrne, D. B., Suarez, G., and McCann, W.R., 1985, Muertos Trough subduction--Microplate tectonics in the northern Caribbean: Nature, v. 317, p. 420-421.

Detrich, C., 1995, Characterization of faults located off the western coast of Puerto Rico using seismic reflection profiles [MS Thesis]: Lehigh University, 122 p.

Dillon, W.P., Edgar, T., Scanlon, K., and Coleman, D., 1996, A review of the tectonic problems of the strike-slip northern boundary of the Caribbean plate and examination by GLORIA, *in* Gardner, J.V. , Field, M.E. and Twichell, D., eds., Geology of the United States' Seafloor; The View from GLORIA, p. 135-164.

Dixon, T., Farina, F., DeMets, C., Jansma, P., Mann, P., and Calais, E., 1998, Relative motion between the Caribbean North American plates and related boundary zone deformation based on a decade of GPS observations: Journal of Geophysical Research v. 103, p. 15157-15182.

Emery, K.O., and Uchupi, E., 1984, The Geology of the Atlantic Ocean, Springer, New York, 1050 p.

Erikson, J., Pindell, J., and Larue, D.K., 1990, Tectonic evolution of the south-central Puerto Rico region: Evidence for transpressional tectonism: Journal of Geology, v. 98, p. 365-386.

Erikson, J., Pindell, J., and Larue, D.K., 1991, Fault zone deformational constraints on Paleogene tectonic evolution in southern Puerto Rico: Geophysical Research Letters, v. 18, p. 569-572.

Gardner, W. O., Glover, and L.K., Hollister, C.D., 1980, Canyons off northwest Puerto Rico: Studies of their origin and maintenance with the nuclear research submarine NR-1: Marine Geology, v. 37, p. 41-70.

Garrison, L.E., and Buell, M.W., 1971, Sea-floor structure of the Eastern Greater Antilles, *in* Symposium on Investigations and Resources of the Caribbean Sea and Adjacent Regions, p. 241-245, UNESCO, Paris, France.

Glover, L., and Mattson, P., 1960, Successive thrust and transcurrent faulting during the early Tertiary in south-central Puerto Rico, Short Papers in the Geological Sciences, U.S. Geological Survey Professional Paper 400-B, p. 363-365.

Glover, Lynn, III, 1971, Geology of the Coamo area, Puerto Rico, and its relation to the volcanic arc-trench association. U. S. Geological Survey Professional Paper 636, 102 p.

Grindlay, N.R., Mann, P., and Dolan, J., 1997, Researchers investigate submarine faults north of Puerto Rico: Eos, Transactions American Geophysical Union, v. 78, p. 404.

Grove, K., 1983, Marine Geologic Map of the Puerto Rico insular shelf, northwestern area-Rio Grande de Añasco to Rio Camuy. U.S. Geological Survey Miscellaneous Investigations Series Map I-1418, 1:40,000.

Hippolyte, J-C., Mann, P. and Grindlay, N.R., 2004, Geologic evidence for the prolongation of active normal faults of the Mona rift into northwestern Puerto Rico, *in* Mann, P., ed., Active

Tectonics and Seismic Hazards of Puerto Rico, the Virgin islands, and Offshore Areas, Geological Society of American Special Paper, this volume.

Huerfano, V., 1997. Crustal structure and stress regime near Puerto Rico, [MS Thesis]: Mayaguez, University of Puerto Rico, p.

Hubbard, D.K., Gill, I.P., Ruebenstone, J.L., and Fairbanks, R.G., 1996, Paleoclimate and paleoceanographic controls of shelf-edge reef development in Puerto Rico and the Virgin Islands, Geological Society of America, Abstracts with Programs, v. 28, p. 489.

Jansma, P., Mattioli, G., Lopez, A., DeMets, C., Dixon, T., Mann, P., and Calais, E., 2000, Neotectonics of Puerto Rico and the Virgin Islands, northeastern Caribbean, from GPS geodesy: Tectonics v. 19, p. 1021-1037.

Joyce, J., McCann, W.R., and Lithgow, C., 1987, Onland active faulting in the Puerto Rico platelet [abs.]: Eos (Transactions, American Geophysical Union), v. 68, p.1483.

Larue, D. K., and Ryan, H.F., 1990, Extensional tectonism in the Mona Passage, Puerto Rico and Hispaniola: A preliminary study: Transactions 12th Caribbean Geological Conference, p. 223-230.

Larue, D.K., Joyce, J., and Ryan, H.F., 1990, Neotectonics of the Puerto Rico Trench: Extensional tectonism and forearc subsidence: Transactions 12th Caribbean Geological Conference, p. 231-247.

Lopez, A., Jansma, P., Calais, E., Demets, C., Dixon, T., Mann, P., and Mattioli, G., 1999, Microplate tectonics along the North American-Caribbean plate boundary: GPS geodetic constraints on rigidity of the Puerto Rico-Northern Virgin Islands (PRVI) block, convergence across the Muertos Trough, and extension in the Mona Canyon [abs.], Eos (Transactions American Geophysical Union), v. 82, p. S77.

Mann, P., Schubert, C., and Burke, K., 1990, Review of Caribbean neotectonics. *in* Dengo, G. and Case, J., eds., The Geology of North America, The Caribbean Region, v. H, p. 307-337.

Mann, P., Taylor, F.W., Edwards, R.L., and Ku, T.L., 1995, Actively evolving microplate formation by oblique collision and sideways motion along strike-slip faults: An example from the northeastern Caribbean plate margin: Tectonophysics, v. 246, p. 1-69.

Mann, P., Calais, E., Ruegg, J-C, DeMets, C., Jansma, P. and Mattioli, G., 2002, Oblique collision in the northeastern Caribbean from GPS measurements and geological observations: Tectonics, v. 21, no. 6, 1057, doi:10.1029/2001TC001304.

Mann, P., Prentice, C., Hippolyte, J.C., Grindlay, N., Abrams, L., and Lao-Davila, D., 2004, Reconnaissance study of Late Quaternary faulting along Cerro Goden fault zone in western Puerto Rico, *in* Mann, P., ed., Active Tectonics and Seismic Hazards of Puerto Rico, the Virgin islands, and Offshore Areas, Geological Society of American Special Paper, this volume.

Masson, D. G. and Scanlon, K. M., 1991, The neotectonic setting of Puerto Rico: Geological Society of America Bulletin, v. 103, p. 144-154.

McCann, W.R., and Sykes, L., 1984, Subduction of aseismic ridges beneath the Caribbean plate: implications for the tectonics and seismic potential of the northeastern Caribbean: Journal of Geophysical Research, v. 89, p. 4493-4519.

McCann, W. R., 1985, On the earthquake hazards of Puerto Rico and the Virgin Islands: Bulletin of the Seismological Society of America, v. 75, p. 251-262.

McCann, W.R., Joyce, J., Lithgow, C., 1987. The Puerto Rico platelet at the northeastern edge of the Caribbean plate [abs.]: Eos (Tansactions American Geophysical Union), v. 68, p. 1483.

Meltzer, A., 1998, Fault structure and earthquake potential Lajas Valley, SW Puerto Rico: U.S. Geological Survey Technical Abstract: http://erp-web.er.usgs.gov/reports/abstracts/1998/ni/g2501.htm.

Meltzer, A., and Almy, C., 2000, Fault structure and earthquake potential Lajas Valley, SW Puerto Rico [abs.]: Eos (Transaction American Geophysical Union), v. 81, p. F1181.

Mercado, A., and McCann, W.R., 1998, Numerical Simulation of the 1918 Puerto Rico Tsunami: Natural Hazards, v.18, p. 57-76.

Molnar, P. .Sykes, L., 1969, Tectonics of the Caribbean and Middle America regions from focal mechanisms and seismicity: Geological Society of America Bulletin, v. 80, p. 1639-1670.

Moya, J. C., and McCann, W.R., 1992, Earthquake vulnerability study of the Mayagüez area, western Puerto Rico: Comision de Seguridad contra Terrmotos, Department of Natural Resources, Puerto Rico, 43p.

Moya, J.C., 1994, Geological, geomorphical and geophysical evidence for paleoseismic events in western Puerto Rico: Proceedings of the Workshop on Paleoseismology, U.S. Geological Survey Open File Report 94-568, p. 127.

Prentice, C., and Mann, P., 2004, Paleoseismic study of the South Lajas fault: First documentation of an onshore Holocene fault in Puerto Rico, *in* Mann, P., ed., Active Tectonics and Seismic Hazards of Puerto Rico, the Virgin islands, and Offshore Areas, Geological Society of American Special Paper, this volume.

Moussa, M.T., Seiglie, G.A, Meyerhoff, A.A., and Taner, I., 1987, The Quebradillas Limestone (Miocene-Pliocene), northern Puerto Rico, and tectonics of the northeastern Caribbean margin: Geological Society of America Bulletin, v. 99, p. 427-439.

Reid, H., and Taber, S., 1919, The Puerto Rico Earthquakes of October-November 1918: Bulletin of the Seismological Society of America, v. 9, p. 95-127.

Schlee, J.S., Rodriguez, R.W., Webb, R.M., and Carlo, M.A., 1999, Marine geologic map of the southwestern insular shelf of Puerto Rico--Mayagüez to Cabo Rojo. U.S. Geological Survey Geologic Investigations Series Map I-2615, 1:40,000.

van Gestel, J-P, Mann, P., Dolan, J., and Grindlay, N.R., 1998, Structure and tectonics of the upper Cenozoic Puerto Rico-Virgin Islands carbonate platform as determined from seismic reflection studies: Journal of Geophysical Research, v. 103, p. 30,505-30,530.

van Gestel J-P, Mann, P., Grindlay, N.R., and Dolan, J.F., 1999, Three-phase tectonic evolution of the northern margin of Puerto Rico as inferred from an integration of seismic reflection, well, and outcrop: Marine Geology, v. 161, p. 259-288.

Western Geophysical Company of America, and Fugro, Inc., 1973, Geological-geophysical reconnaissance of Puerto Rico for citing of nuclear power plants. The Puerto Rico Water Resources Authority, San Juan, P.R., 127p.

TABLE CAPTIONS

Table 1. Processing steps for SCS data.

FIGURE CAPTIONS

Figure 1. Tectonic setting of the northeastern Caribbean region. Plate vectors relative to a fixed North American plate from Mann et al., 2002. Focal Mechanisms from Havard CTM database, Molnar and Sykes (1969) and Heurfano (1997). Epicenters of recent large magnitude earthquakes in the region also labeled with year of occurrence (NEIC PDE database). GNPRFZ = Great Northern Puerto Rico Fault Zone, GSPRFZ = Great Southern Puerto Rico Fault Zone, SFZ = Septentrional Fault Zone.

Figure 2. Shaded relief map of the island of Puerto and offshore region. Major structural lineaments and faults shown by heavy black lines. Faults in Mona Passage identified by Grindlay et al. (1997) and van Gestel et al. (1998). Structural lineaments onland from Glover (1971). Digital elevation model created from U.S. Geological Survey 3 arc second DEM for Puerto Rico and NOAA hydrographic data. Location of the 1918 earthquake shown by filled circle. Boxed area shows coverage of Figure 3. Inferred axis of E-W trending arch shown as dashed thick grey line.

Figure 3. Shaded relief map of western Puerto Rico and offshore region. Ship tracks for May 2000 survey shown in thin red lines. Trackline for a portion of MCS line ID-131-D (Fig. 4) is shown as dashed line. The four boxes represent coverage area of maps shown in figures 5, 8, 10 and 12. Location of the Cerro Goden fault zone determined from McIntyre (1971) and Mann et

al. (this volume) and location of South Lajas fault from Glover (1970), Meltzer et al. (1998; 2000), and Prentice and Mann (this volume). Dashed line with question marks is the hypothesized eastward extension of the Cordillera fault. Serpentinite bodies mapped onland are shown as areas with striped fill pattern. Inferred axis of E-W trending anticline formed during early Pliocene N-S shortening event shown as dashed thick black line.

Figure 4. a and b) Western Geophysical MCS line ID131-D reprocessed including migration from Detrich (1995). This MCS line parallels the west coast of Puerto Rico (see inset for location) and clearly shows north dipping reflectors truncated by high-angle, normal faults (dashed lines), forming several structural basins. The north dipping reflectors are interpreted to be the Oligocene-Pliocene carbonate platform that experienced deformation associated with a north-south shortening episode post-early Pliocene. The profile shown is located along the north-dipping limb of a regional arch developed during Phase 2 (e.g., Mann et al. (this volume) fig 14d). Boxes show location of seismic profiles shown in figures 7 and 9 that parallel this MCS line and image similar features. The large normal faults appear co-incident with seafloor features identified in this study that define the Cerro Goden fault zone (CGFZ), Punta Algarrobo/Mayagüez fault zone (PA/MFZ), Punta Guanajibo fault zone (PGFZ), and Punta Arenas fault zone (PAFZ). b) Three-Dimensional shaded relief perspective of western Puerto Rico looking eastward combined with MCS line ID131-D. Illumination is from the northwest.

Figure 5. Sidescan sonar mosaic of North Añasco Bay (Fig. 3 shows location). Location of seismic profiles indicated by thick solid lines. MCS tracks are ID-131-D, XI-108-D and I-129-D, SCS tracks are L37 and L41. MCS profiles ID-131-D and I-129-D extend beyond southern

boundary of figure. Dashed lines mark location of linear features visible in sidescan sonar mosaic, seafloor offsets in SCS profiles and offsets of deeper structures in MCS profiles projected to the seafloor. These features are interpreted as offshore extensions of the Cerro Goden fault zone (CGFZ). F1, F2 and F3 mark the location of semi-continuous fault traces within the CGFZ. Earthquake epicenters (NEIC PDE database 1973-2000) of earthquakes with magnitudes >2.5 shown as filled circles. Bathymetry contour interval=10 m, and 1 m-pixel resolution mosaic. Imagery within boxed area is shown in figure 6 and dashed box area is enlarged and shown as an inset. Reefs enclosed by dashed lines appear to be offset by ~ 350-400m right-laterally(F2). F3 identified on SCS lines is not apparent on MCS lines XI-108-D (Fig. 7) or ID-131-D (Fig. 4).

Figure 6. a) Sidescan sonar enlargement (Fig. 5) showing terraces labeled "A" and "B" and a portion of the CGFZ including F1 and F2 as in Fig. 5. b) SCS Line 33 showing the two terraces at ~80 m and ~40 m formed by sea-level stillstands or slow downs during the most recent transgression (depth scale assumes V=1500 m/s). c) Map view showing SCS line 33 (solid line), terraces as dotted lines and fault traces making up the CGFZ as dashed lines.

Figure 7. a and b) SCS profiles across the CGFZ (depth scale assumes V=1500 m/s). Approximately 20-25 m of sediment fills depressions between exposed reef heads. Acoustic basement in these profiles is interpreted as the boundary between alluvium (Holocene?) and well indurated sediments and sedimentary rocks. Offsets (dashed lines) of seafloor and offsets and tilting of sediments indicates recent fault displacement. c) MCS Line XI-108-D shows offset (dashed line) of the Oligocene-Pliocene carbonate platform and overlying section which is

assumed to be Pliocene and younger in age. The trace of this normal fault projected to the seafloor aligns with fault (F2). Note that fault F3 is not associated with any deep structure imaged. d) Map view showing MCS and SCS tracklines (solid lines) and the fault segments within the CGFZ (dashed lines).

Figure 8. (two facing pages) Sidescan sonar mosaic of the North Mayagüez Bay area (Fig. 3 shows location). Location of MCS tracklines indicated by thick solid lines and SCS line 104 shown as dotted line. Dashed lines indicate location of linear features visible in sidescan sonar mosaic, seafloor offsets in SCS profiles and offsets of deeper structures in MCS profiles projected to the seafloor. These features locate the Punta Algarrobo and Mayagüez fault zones (PA/MFZ). Short black arrows indicate location and direction of sediment transport from the Añasco Basin into the Mayagüez Basin. Earthquake epicenters (NEIC PDE database 1973-2000) of earthquakes with magnitudes >2.5 shown as filled circles. Bathymetry contour interval=10 m, and 1 m-pixel resolution mosaic.

Figure 9. Coincident SCS and MCS profiles across the Punta Algarrobo and Mayagüez fault zones (PA/MFZ) in Mayagüez Bay. a) SCS line 104 shows that the high angle normal fault imaged in MCS creates south facing scarps and truncates north dipping reflectors, which outcrop at the seafloor or are thinly sedimented. Boxed area is enlarged and reveals an offset in the seafloor and near surface alluvium accumulating in the Mayagüez Basin. b) MCS line I-129-D clearly shows north dipping reflectors truncated by high-angle, normal faults (dashed lines). The north dipping reflectors are interpreted to be the Oligocene-Pliocene carbonate platform (also see Fig. 4). The boxed area shows the area imaged by SCS line 104. c) Map view showing tracklines

of MCS (thin solid line) and SCS (thick solid line) profiles and the fault segments comprising the PA/MFZ (dashed lines).

Figure 10. Sidescan sonar mosaic of South Mayagüez Bay (Fig. 3 shows location). Thick black lines indicate locations of SCS and MCS profiles. MCS profile ID131-D extends beyond the northern border of figure (Fig. 4). Dashed lines indicate location of linear features visible in sidescan sonar mosaic, seafloor offsets in SCS profiles and offsets of deeper structures in MCS profiles projected to the seafloor. These features locate the Punta Guanajibo and Punta Arenas fault zones (PG/PAZ). Filled pattern locates serpentinite. Earthquake epicenters (NEIC PDE database 1973-2000) of earthquakes with magnitudes >2.5 shown as filled circles. Bathymetry contour interval is 10 m, and 1 m-pixel resolution mosaic. Imagery within boxed area is shown in figure 11.

Figure 11. a) SCS line 134 across the Punata Guanajibo fault zone (PGFZ). Offsets in seafloor and/or surface sediments that are also apparent on adjacent SCS lines are indicated by numbered arrows. Filled arrows number 1, 3, and 4 are offsets that are apparent on both SCS and sidescan sonar records. Well stratified and tilted sediments fill the fault bounded depression b) Enlarged area of sidescan sonar mosaic from figure 10 showing fault lineaments numbered to correspond with SCS. c) Map view showing SCS trackline (solid lines) and numbered fault segments within the PGFZ (dashed lines). Note that the trend of the PGFZ projects to the Serpentinite belt mapped on shore.

Figure 12. (two facing pages) Sidescan sonar mosaic of Boquerón Bay area. Thick solid lines indicate location of SCS lines 139 and 64 shown in figure 13. Axis of EW trending arch shown as dashed thick black line. South of the axis, reflectors in SCS profiles dip SSW, north of the axis reflectors dips NNE. Filled pattern locates serpentinite. Earthquake epicenters (NEIC PDE database 1973-2000) of earthquakes with magnitudes >2.5 shown as filled circles. Bathymetry contour interval is 10 m, and 1 m-pixel resolution mosaic. Sidescan sonar data were not able to resolve any seafloor displacements offshore of the Lajas valley.

Figure 13. a & b) SCS profiles of Boquerón Bay. South dipping reflections are interpreted as the uppermost portion of the Oligocene-Pliocene carbonate platform. This dip is consistent with structure imaged by offshore MCS profiles. An angular unconformity is apparent between the dipping carbonate strata and the uppermost flat-lying, continuous reflections that are interpreted as Holocene in age. Seafloor or surficial sediment offsets are not observed in any of the SCS profiles offshore of the Lajas valley. c) Map view showing SCS trackline (solid lines). Series of strike and dip symbols for top of the carbonate platform imaged in SCS and MCS indicating location of dipping reflectors projected to the seafloor.

Figure 14. Residual magnetic intensity map for western Puerto Rico (after Bracey, 1968). Contour interval = 50 gammas. Filled pattern locates serpentinite and offshore faults identified by this study and faults with proposed Quaternary activity onland shown by dashed lines. Dashed line with question locates the projection of the cordillera fault along the serpentinite belt to the western coast. Note the correspondence of the Punta Algarrobo/Mayagüez fault zone, the Monte

del Estado peridotite/serpentinite belt onland and shaded zone of low magnetic intensity. CSA = Cordillera de Sabana Alta.

Figure 15. a) Three-dimensional perspective of western Puerto Rico looking eastward. Illumination is from the northwest. Faults identified during this survey are marked as black lines and are tentatively traced to Quaternary faults onland. Faults onland in the vicinity of Aguadilla from Hippolyte et al., (this volume). Also shown is the axis of the east-west trending arch. Note the change in insular shelf morphology south to north from broad, flat and undeformed to relatively narrow, deformed and dissected. CGFZ=Cerro Goden fault zone, PA/MFZ=Punta Algarrobo/Mayagüez fault zone, PG/PAFZ=Punta Guanajibo/Punta Arenas fault zone, SLFZ=South Lajas fault zone.

b) Conceptual model for the neotectonics of the Puerto Rico region. Much of the Quaternary faulting is primarily right-lateral transtension. This extension is the result of differential relative motions (shown by the GPS vectors) both in direction and velocity between the Hispaniola, PRVI and the Caribbean plates.

Processing Steps for Single-Channel Seismic Data
Convert files from SEG-Y format
Spherical Divergence Gain (t^2)
Bandpass Filter: 100-150-1000-1100 Hz
Spectral Whitening: 150-1000 Hz
Digitization of the seafloor
Application of seafloor mute
Trace Mixing: 3 traces, not weighted
Application of AGC: 50 ms

Table 1 - Grindlay et al.,

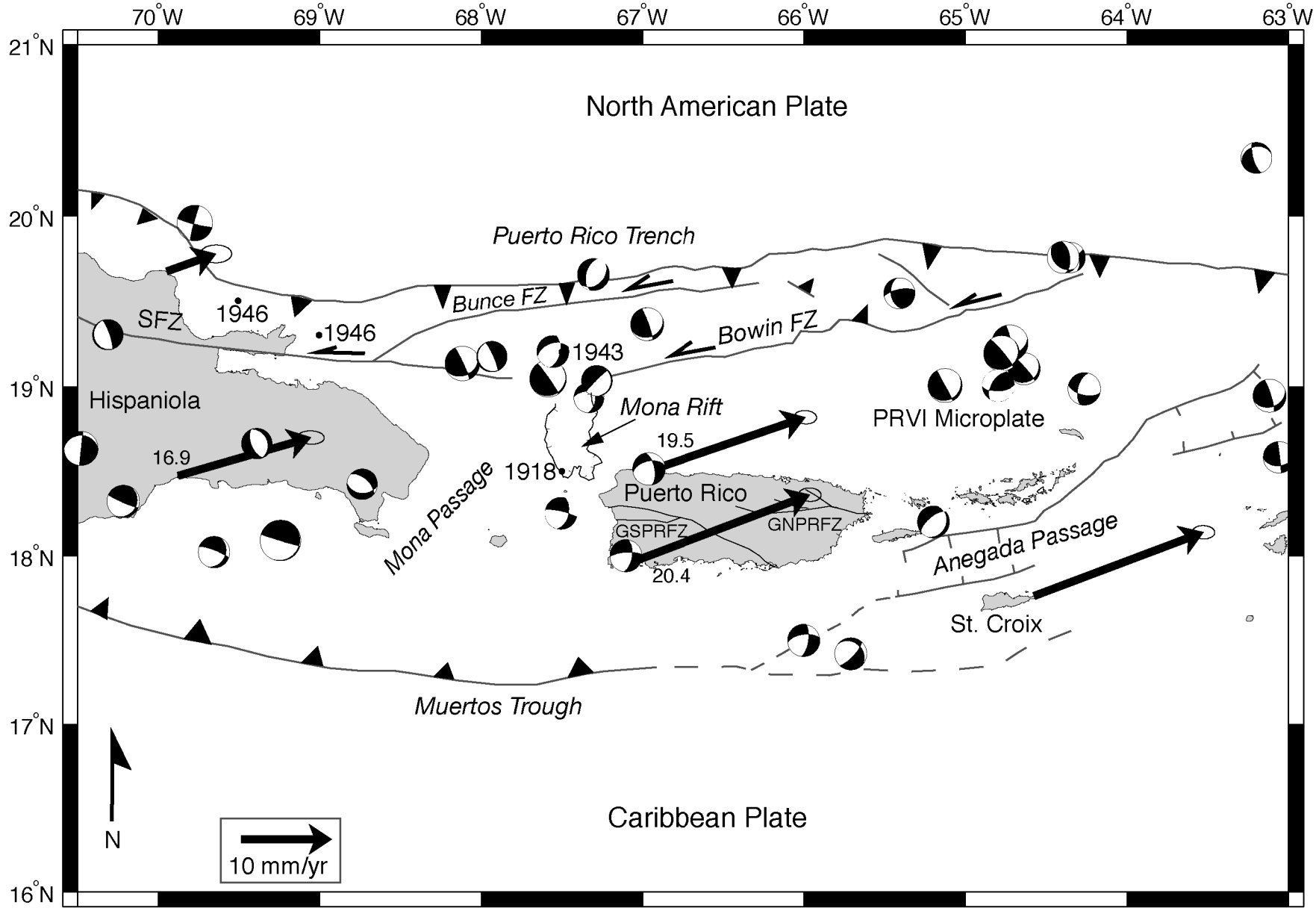

Fig. 1, Grindlay et al.

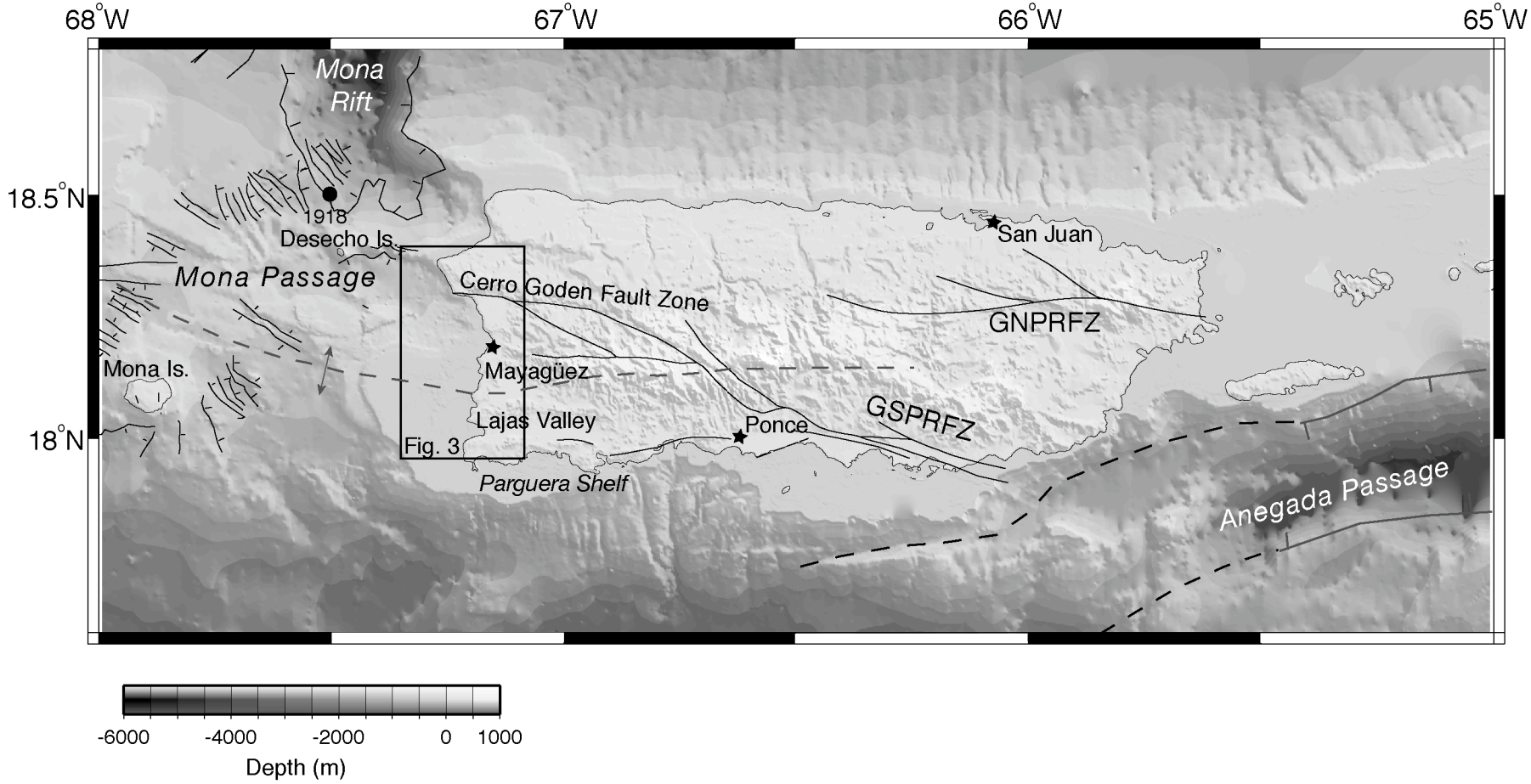

Fig. 2, Grindlay et al.

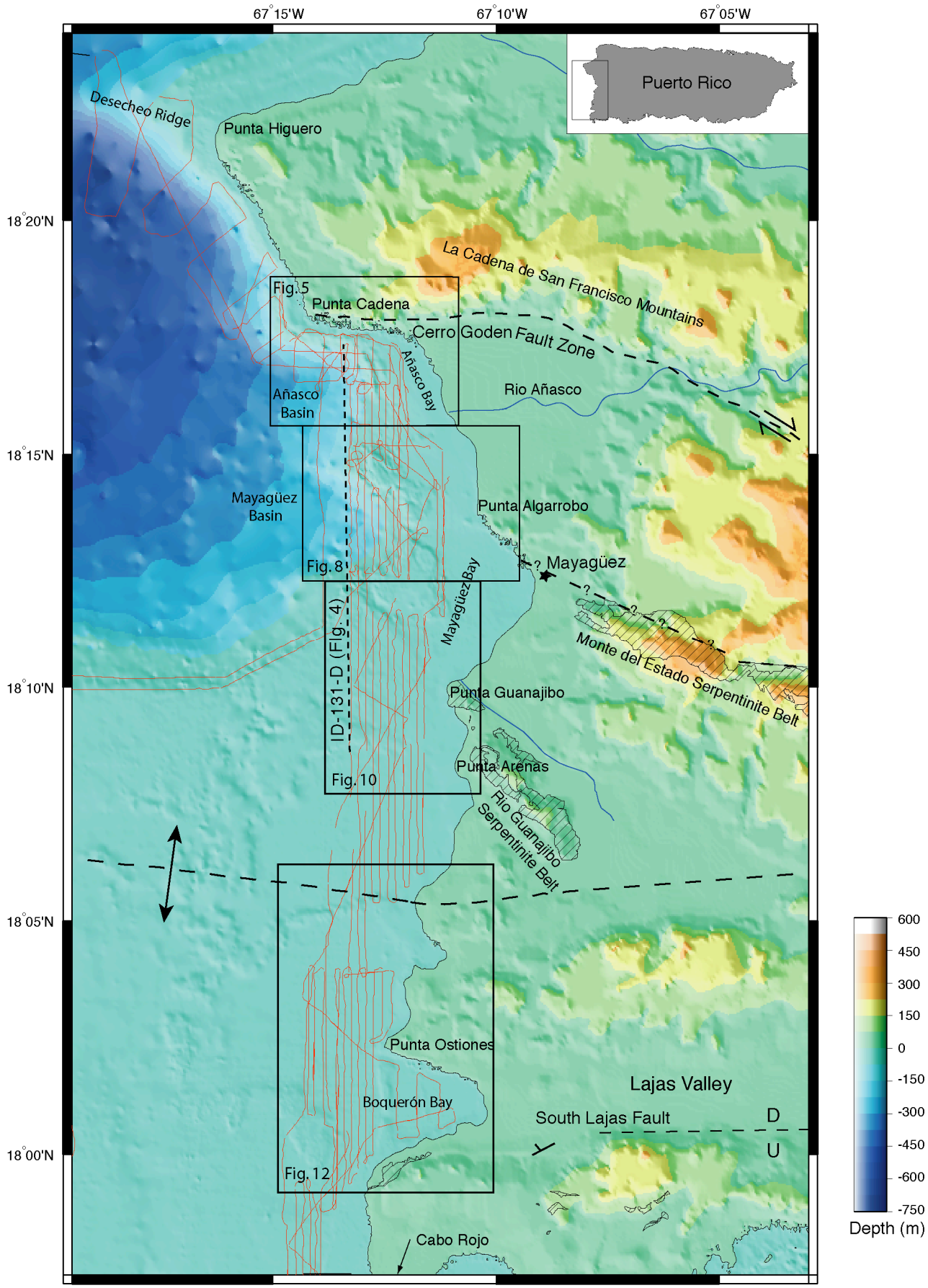

Fig. 3 Grindlay et al.

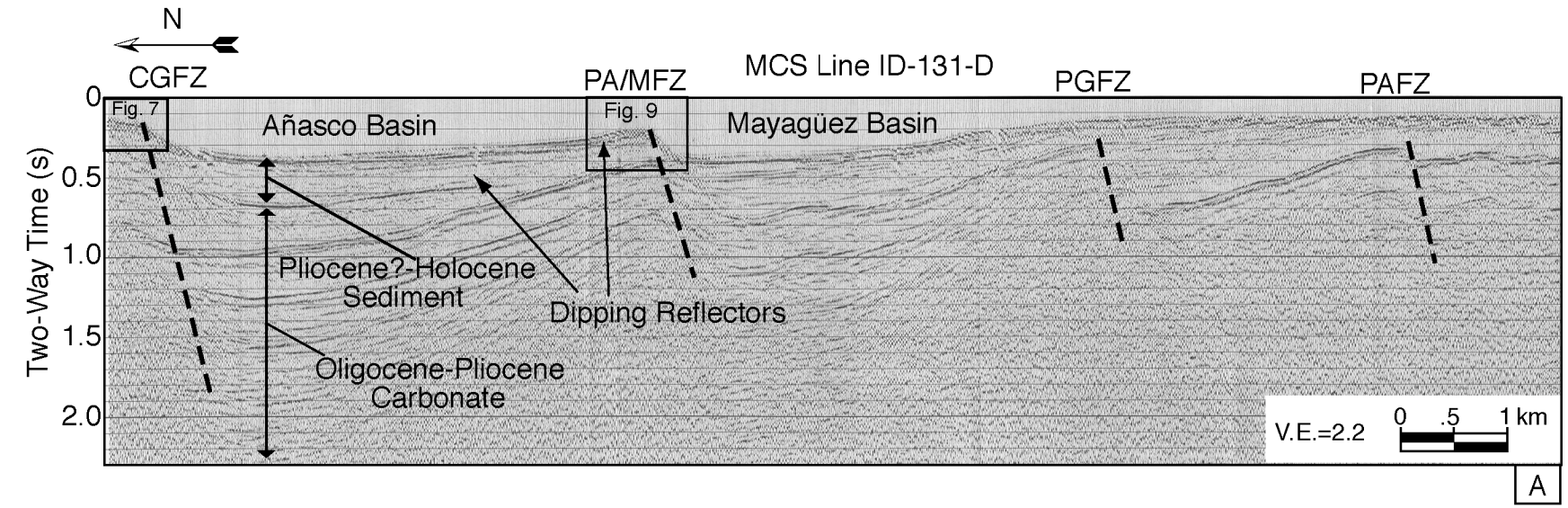

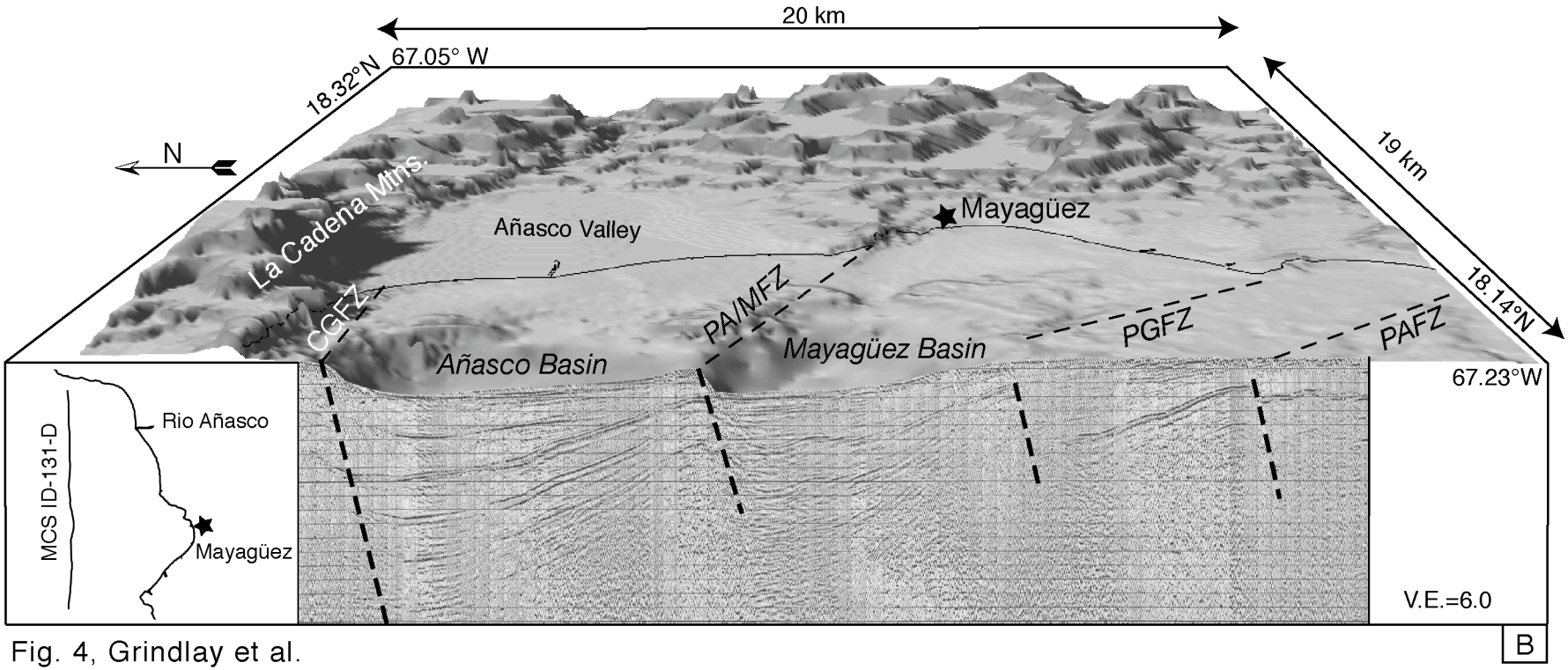

Fig. 4, Grindlay et al.

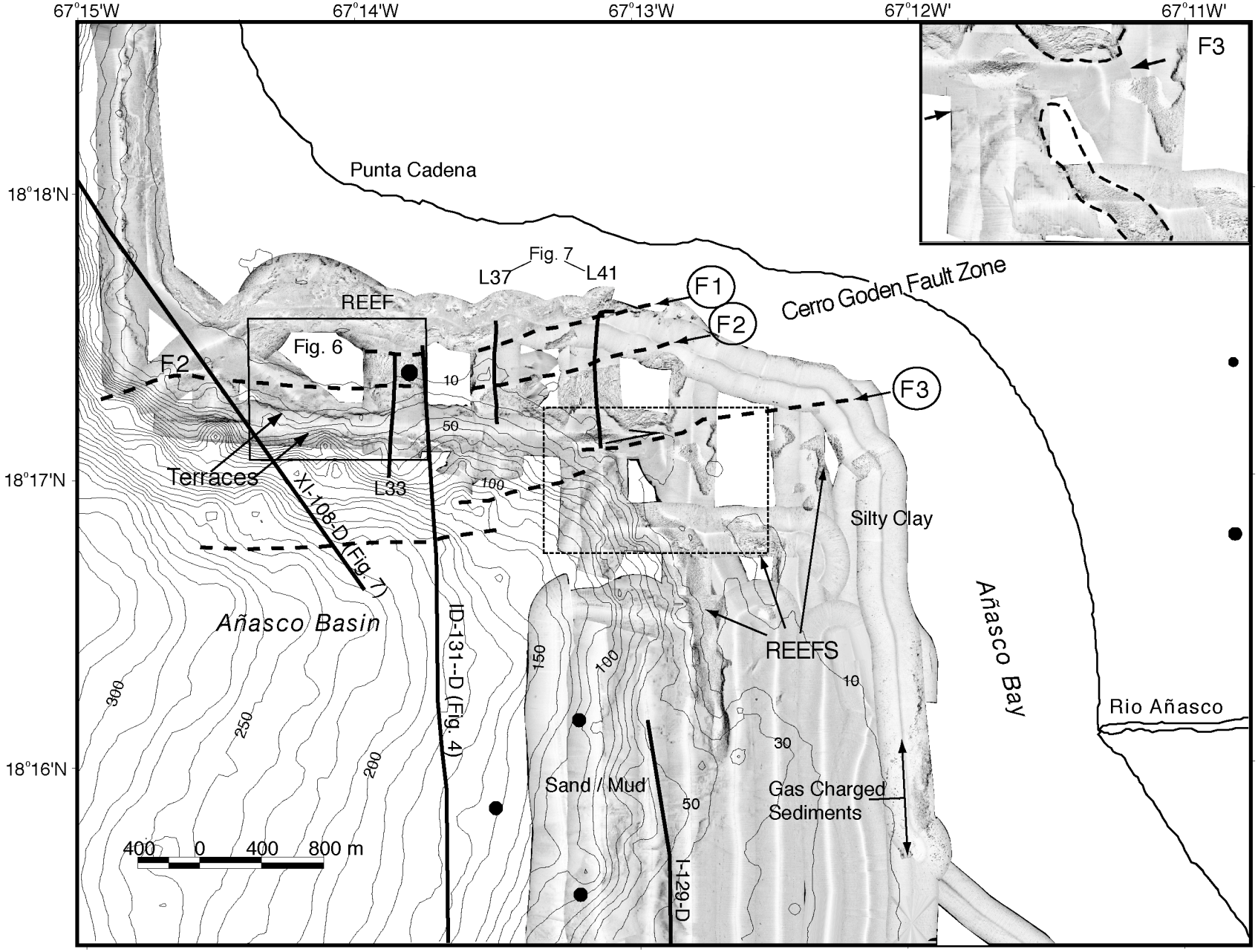

Figure 5, Grindlay et al.

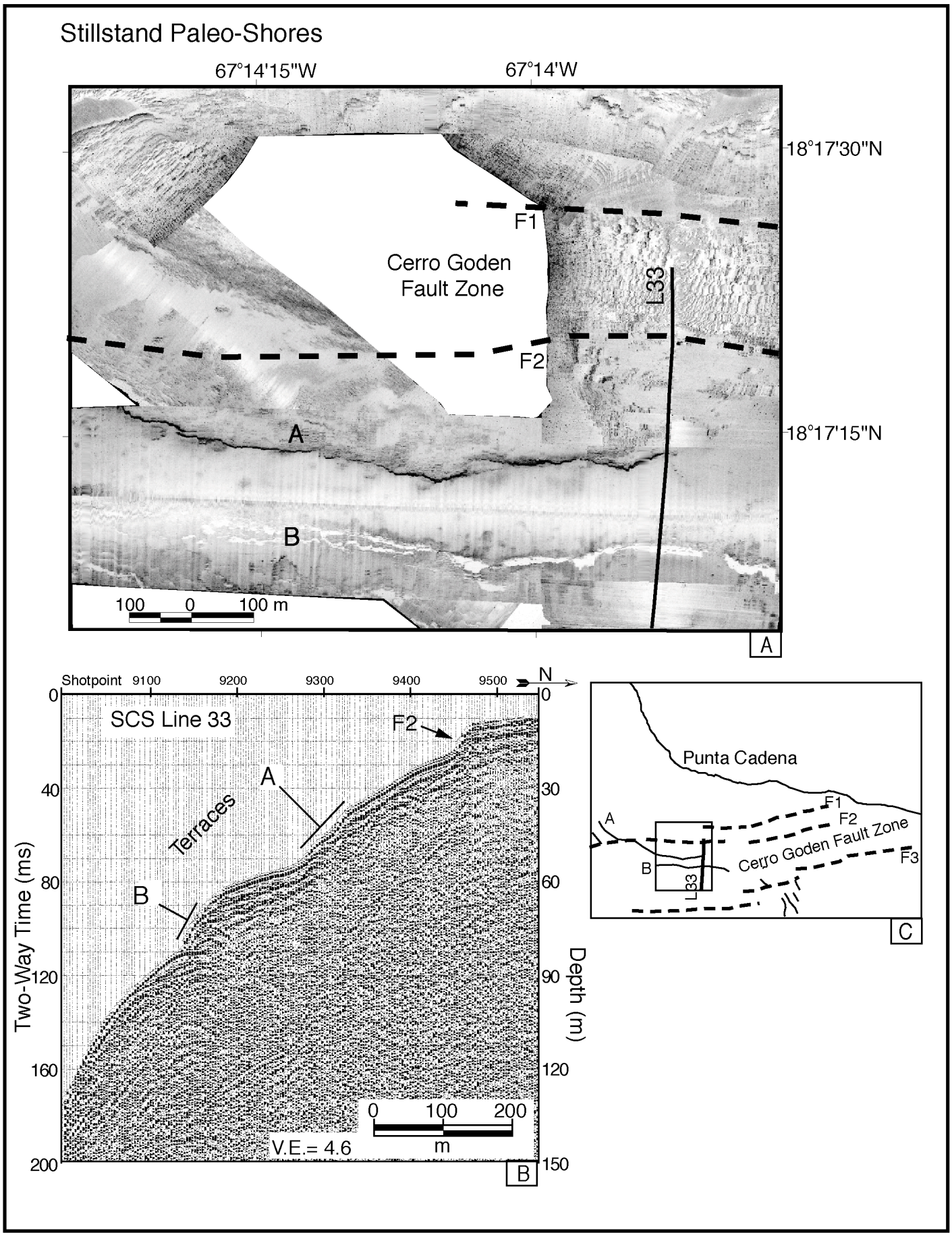

Fig. 6, Grindlay et al.

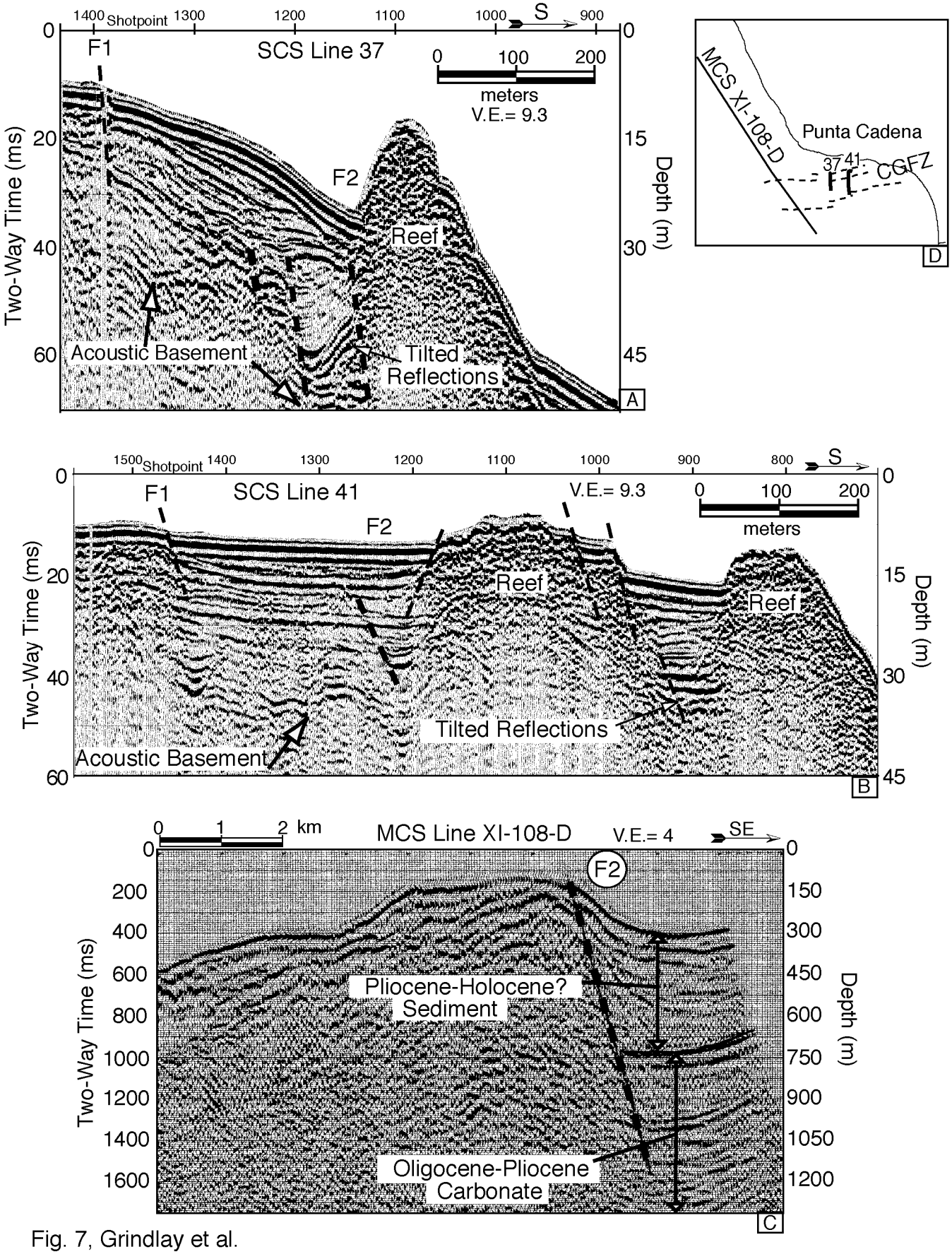

Fig. 7, Grindlay et al.

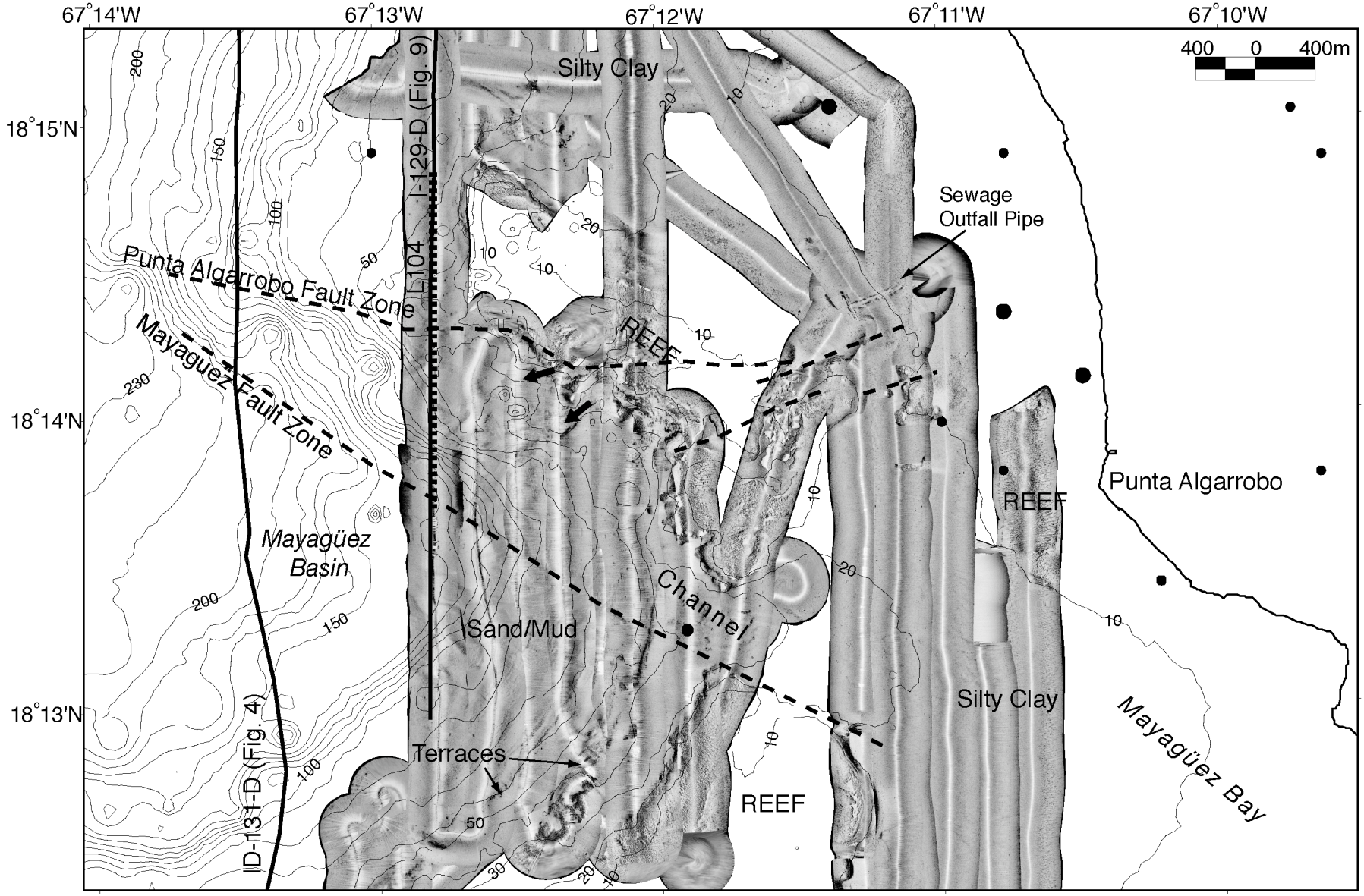

Fig. 8, Grindlay et al.

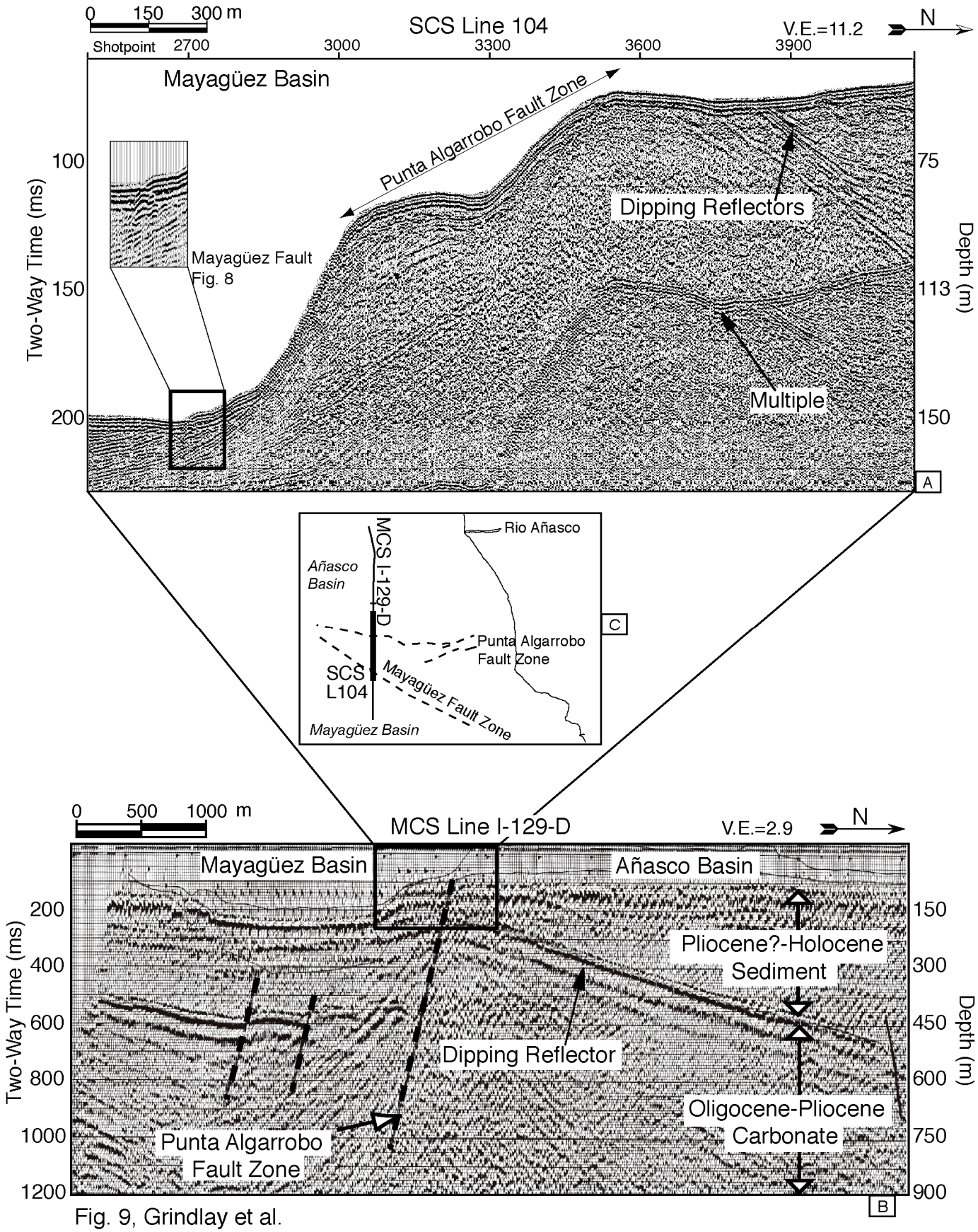

Fig. 9, Grindlay et al.

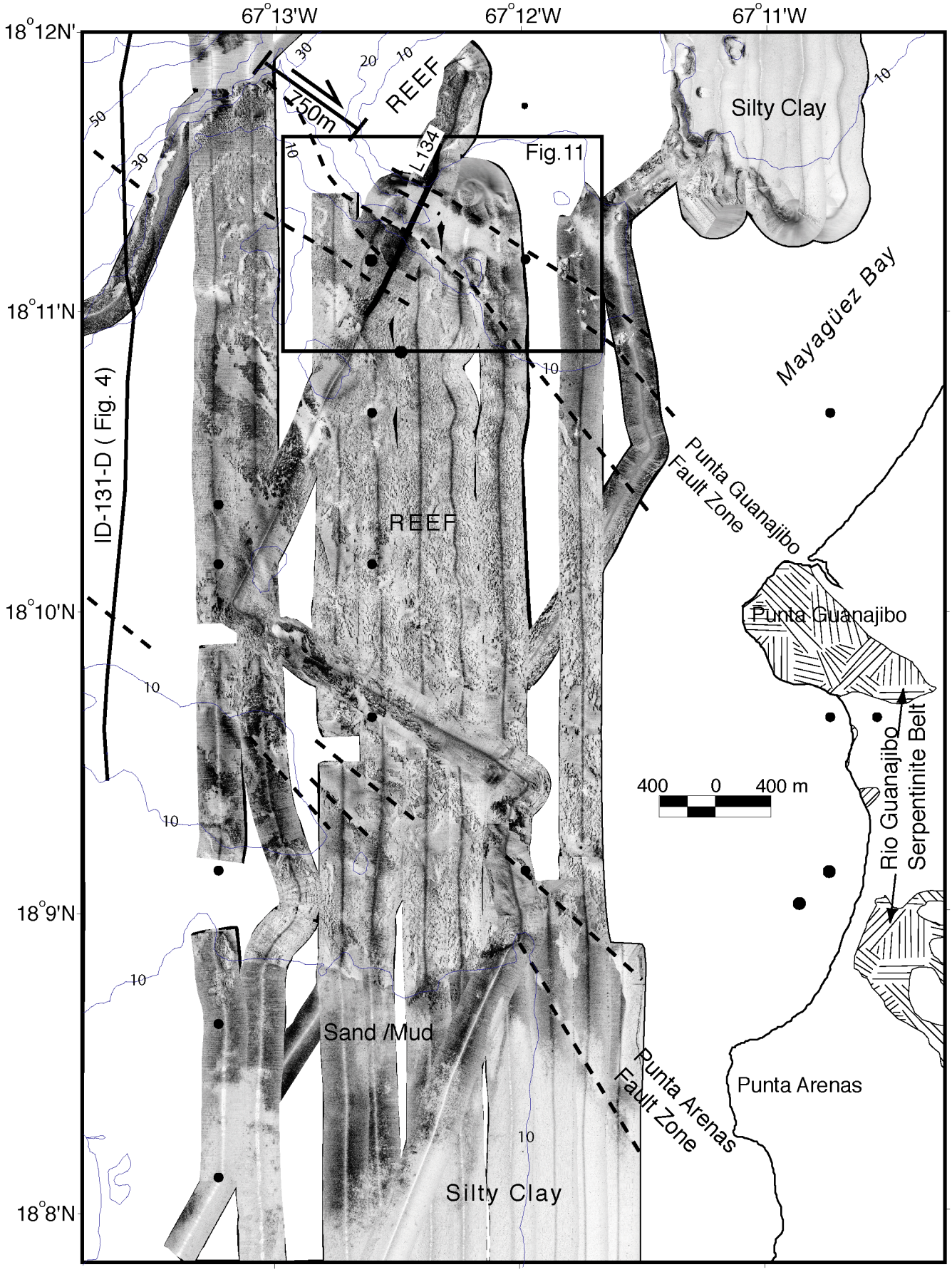

Fig. 10, Grindlay et al.

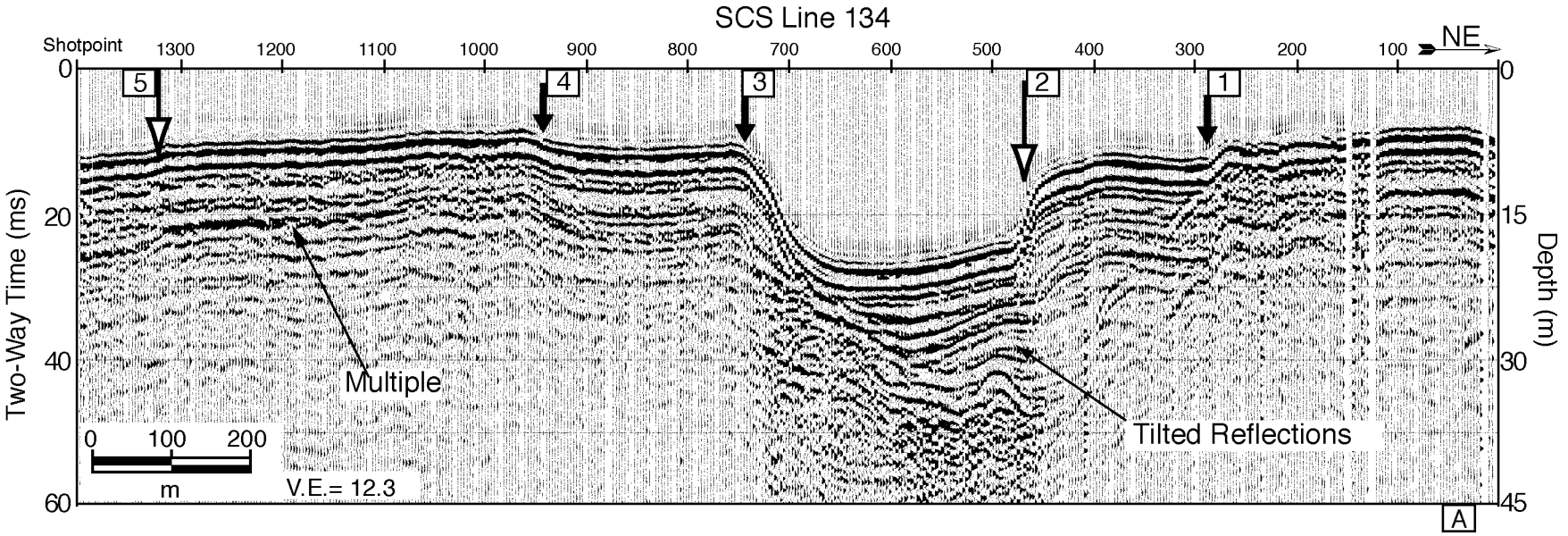

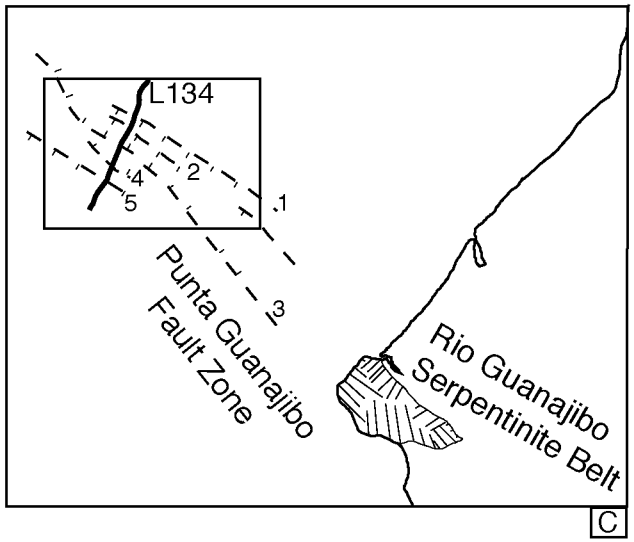

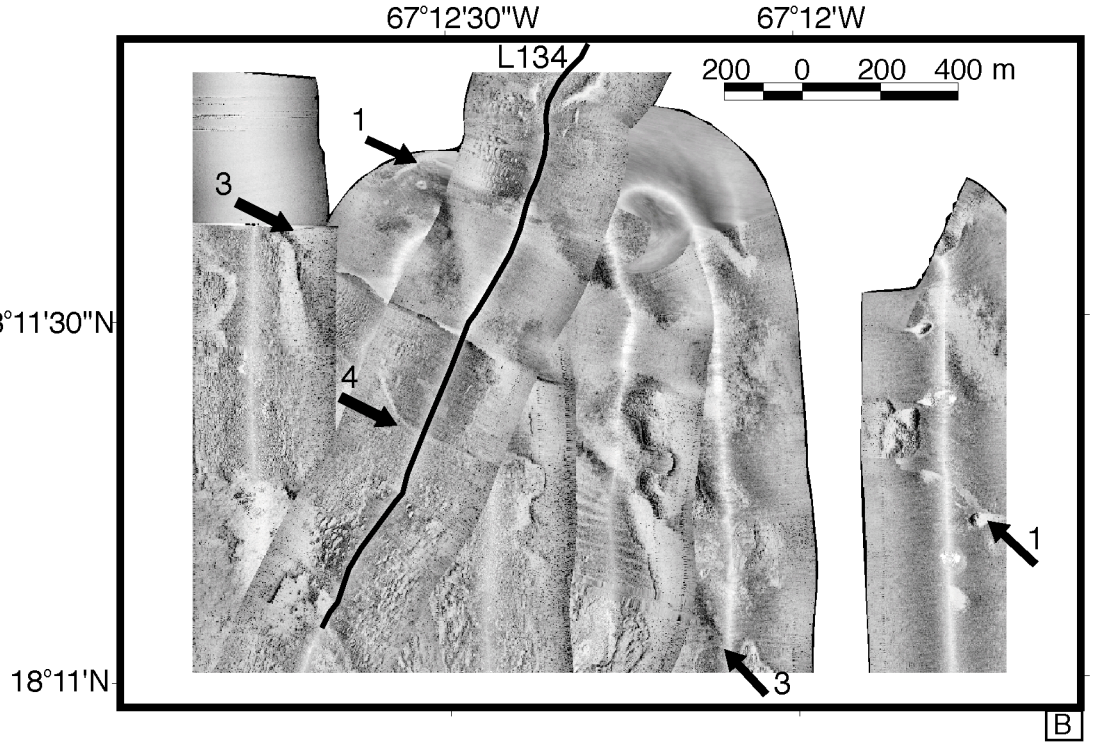

Fig. 11, Grindlay et al.

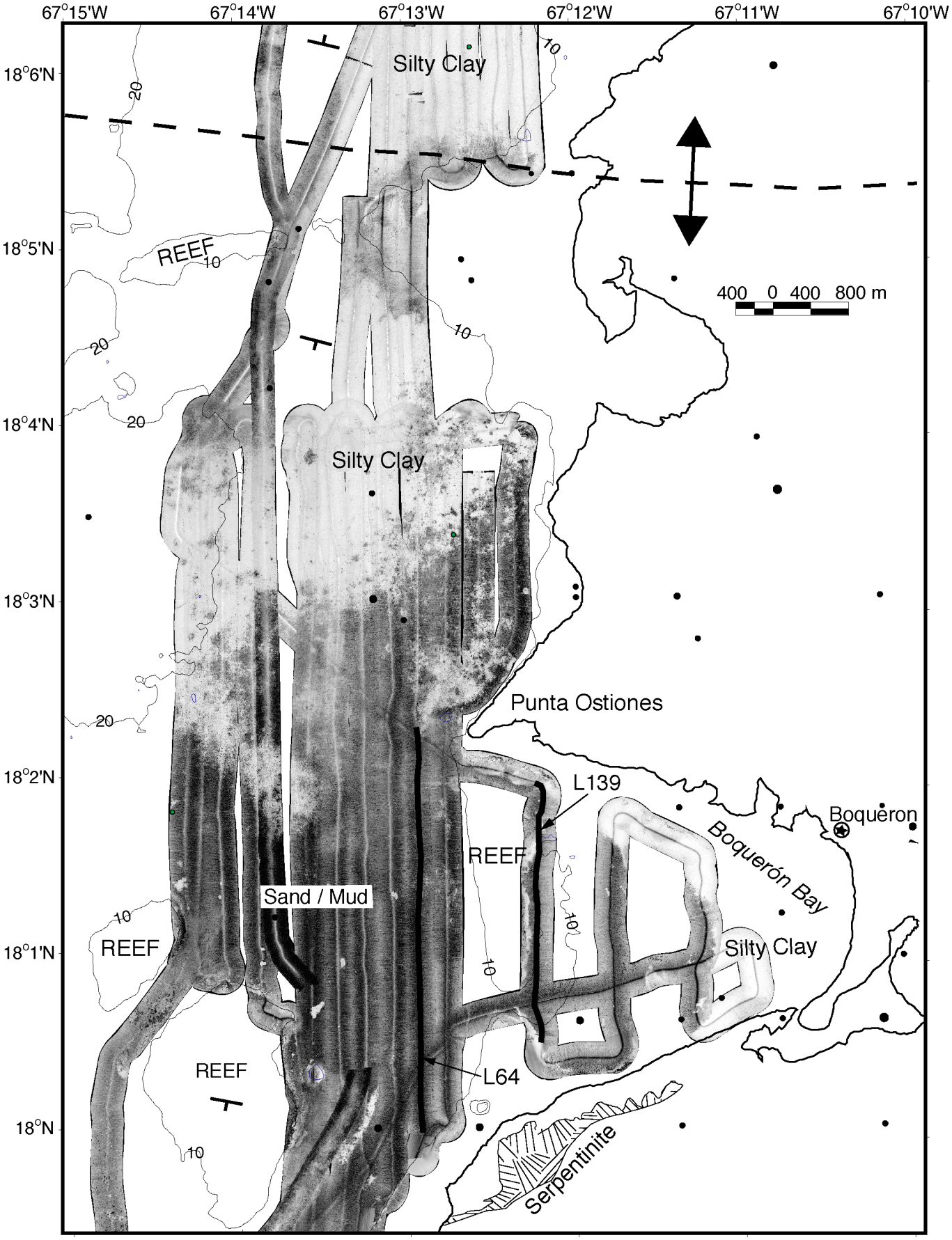

Figure 12, Grindlay et al.

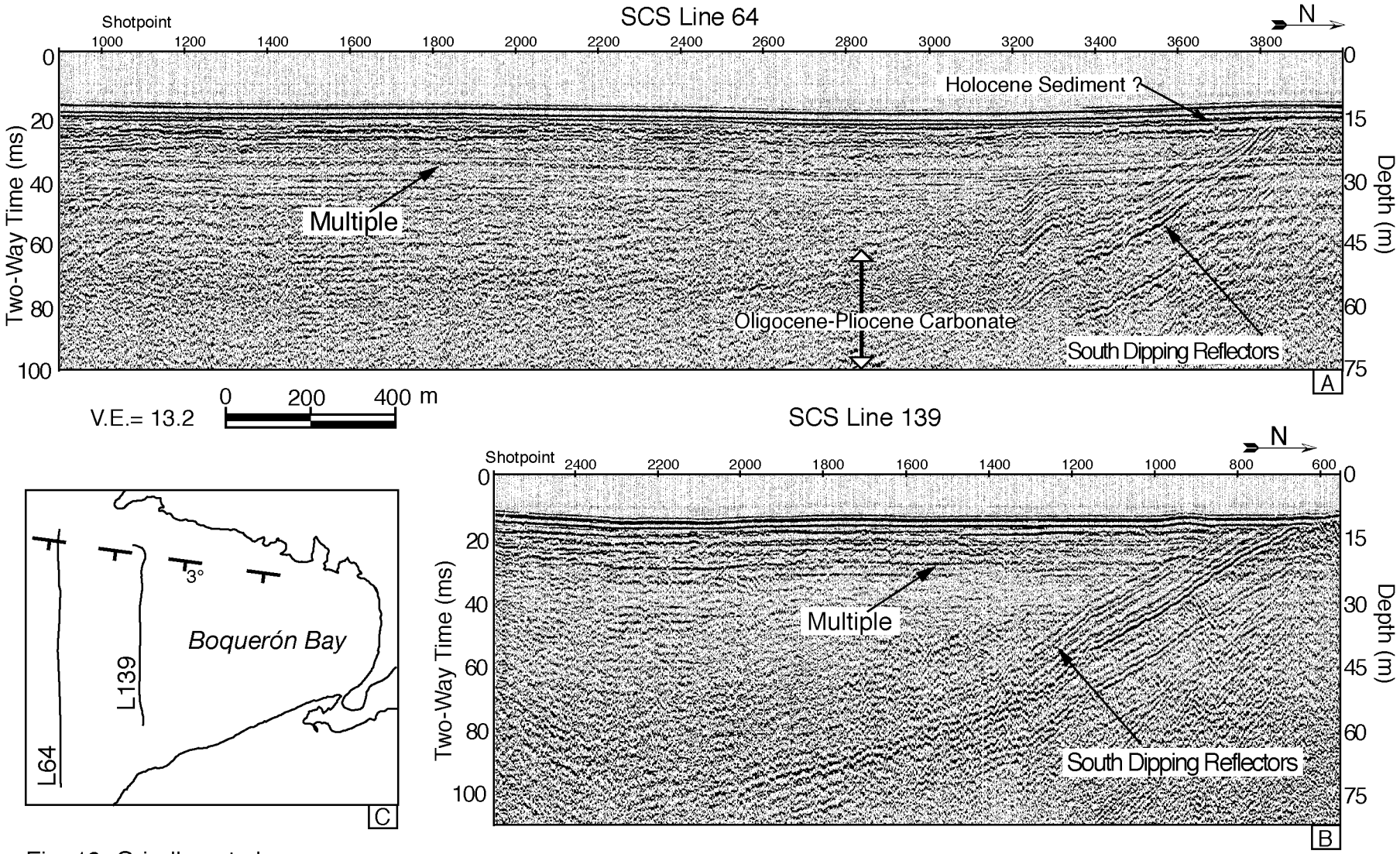

Fig. 13, Grindlay et al.

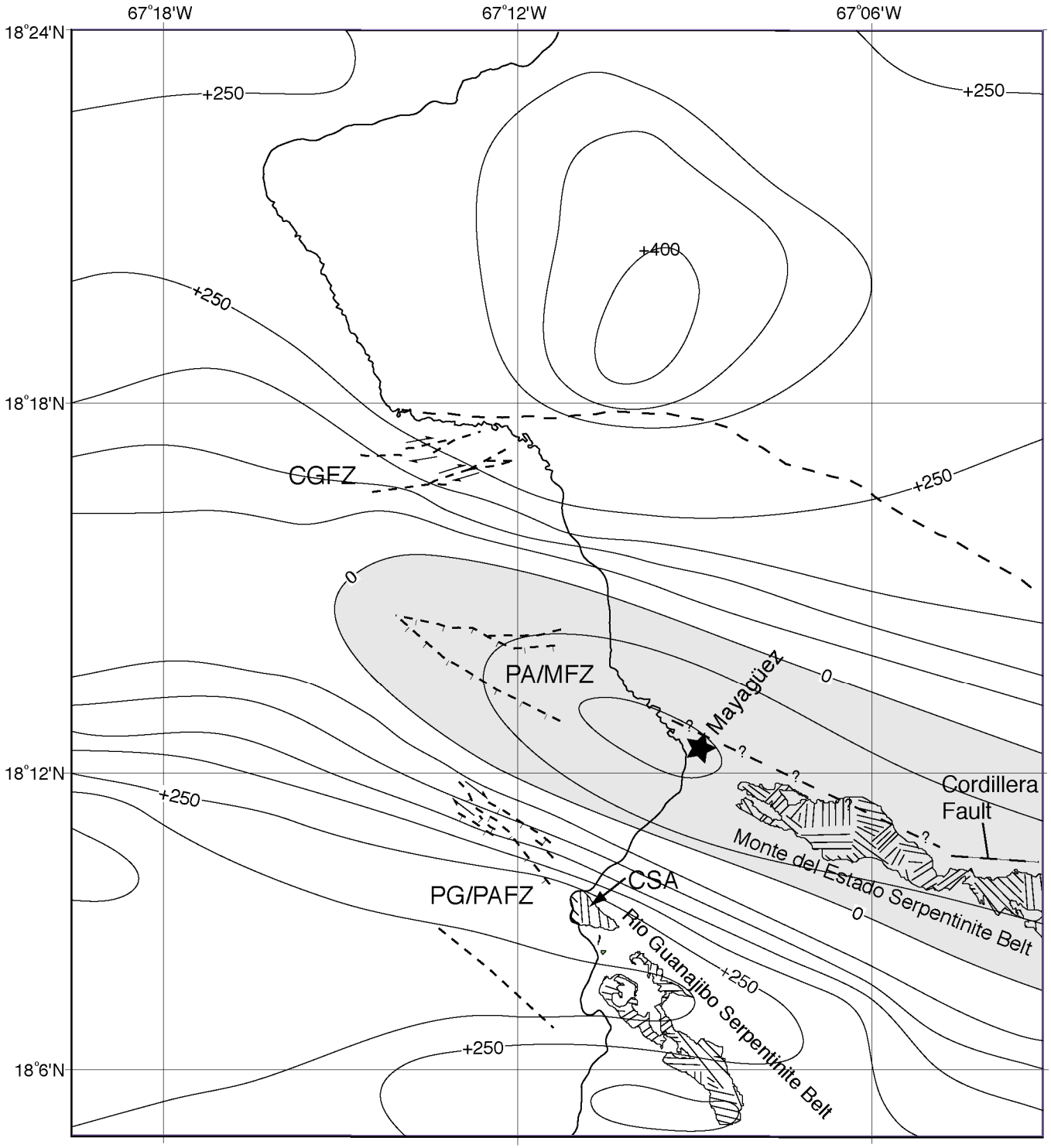

Fig. 14, Grindlay et al.

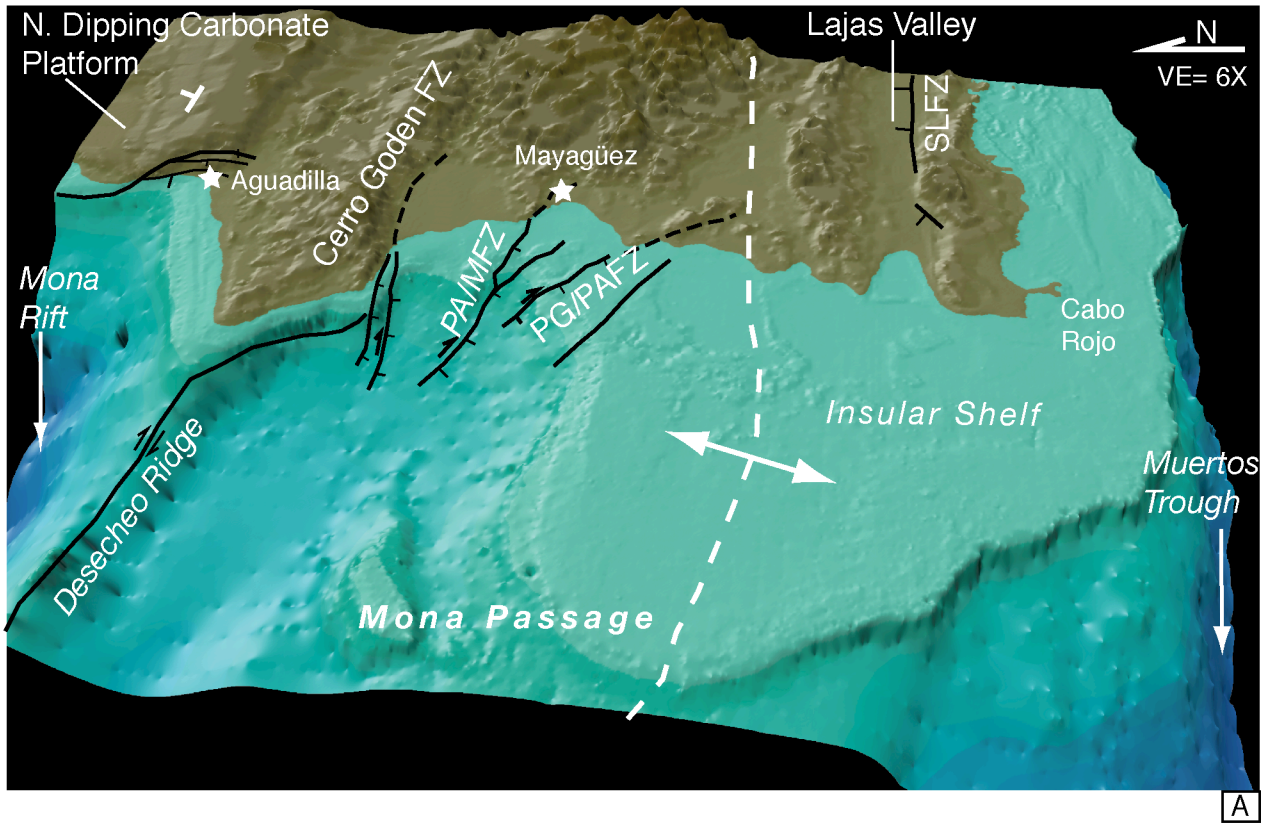

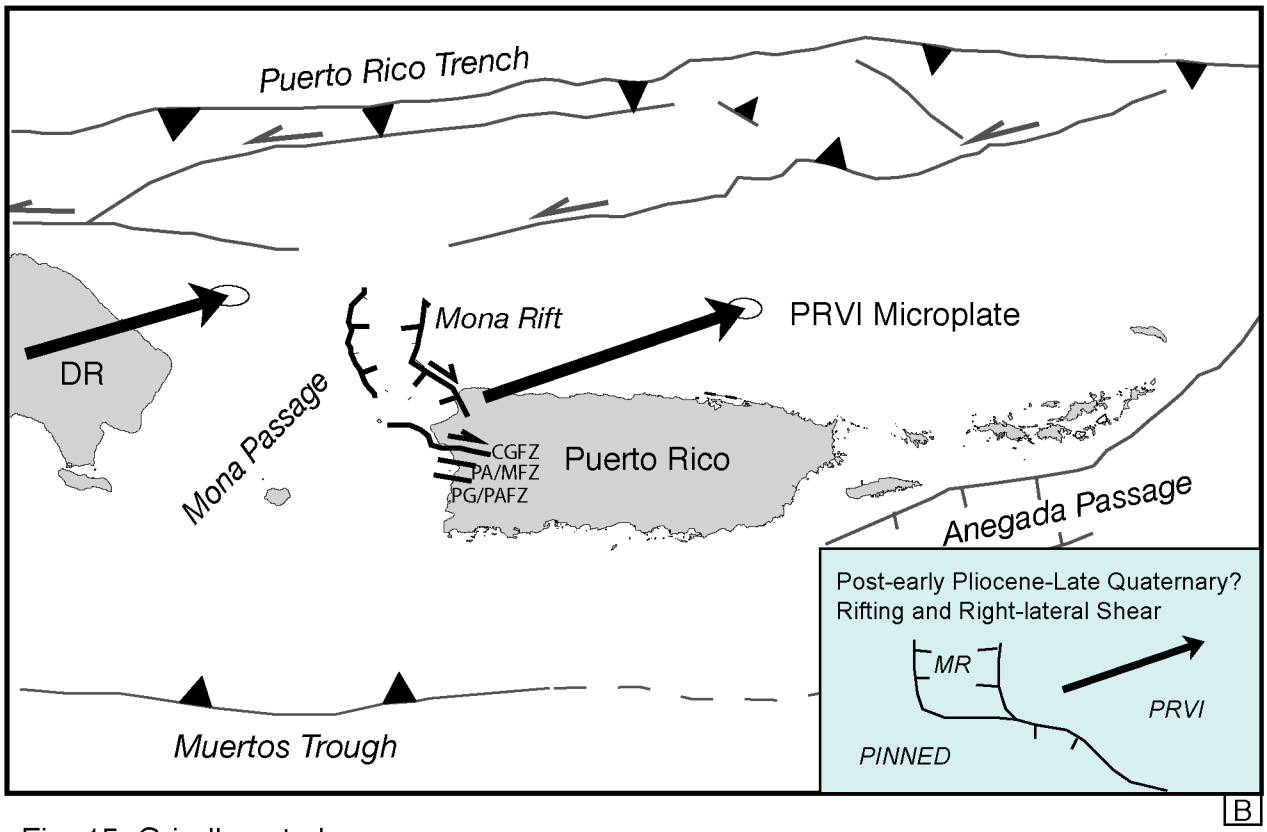

Fig. 15, Grindlay et al.